

Evaluating climate change over the Colorado River basin using regional climate models

Yanhong Gao^a, Julie A. Vano^a, Chunmei Zhu^a, and Dennis P. Lettenmaier^a

Submitted to Journal of Geophysical Research – Atmospheres Revised 3/25/11

^aDepartment of Civil and Environmental Engineering Box 352700, University of Washington, Seattle,
WA 98195, USA

Abstract

We use Regional Climate Model (RCM) simulations from the North American Regional Climate Change Assessment Program (NARCCAP) to evaluate implications of climate change for the discharge of the Colorado River in the mid-21st century. We compare historical RCM simulations and simulations from their host global General Circulation Models (GCMs) to 1/8-degree gridded observations of precipitation, surface air temperature, and runoff (generated by the Variable Infiltration Capacity (VIC) land surface model forced with gridded observations) for the historical period 1970-1999. The RCMs capture the primary features of observations better than their host GCMs in part because of their ability to better represent strong upward lift in topographically complex regions. Although the RCMs do not significantly improve the simulation of precipitation, their ability to better represent surface temperature in mountainous regions has important effects on simulations of evapotranspiration, snowpack, and runoff. In the Colorado River basin, projected mid-21st century runoff changes are mostly impacted by the combination of snow cover change in winter, temperature change in spring, and precipitation change in summer. In particular, the response of cold-season temperatures in headwater streams is key to determining the basin's susceptibility to a warming climate. Due to the cooler temperature and higher snow line in RCMs relative to GCMs, the RCMs project less warming in the spring and thus generate smaller decreases in runoff, both during spring and annually, as compared with GCMs. Changes in surface air temperature, runoff, and snow water equivalent at high elevations all indicate that headwater streams of the Colorado River are less susceptible to a warming climate in climate change simulations that use RCMs than in simulations that use GCMs. Nonetheless, the 50-km NARCCAP grid resolution has some limitations in resolving orographic effects, which suggests that there may remain residual biases in the climatic sensitivity of the RCM simulations.

1.0 Introduction

The Colorado River Basin (CRB) includes parts of seven U.S. states and Mexico (Figure 1). The headwaters lie in the Rocky Mountains of Wyoming and Colorado, where about 75% of annual streamflow is generated from 25% of the area (Hoerling et al., 2009; Franz et al., 2003; Cayan et al., 2001), while the lower basin contributes to only 8% of annual streamflow. With an annual average discharge of roughly 18.5 BCM/yr, the CRB is not particularly large in terms of discharge, especially when compared to other major continental rivers in the U.S., like the Mississippi or Columbia. Still, the Colorado River is the most important source of water for the vast, arid southwestern United States. It provides water to 27 million people in the southwestern U.S. and Mexico (Barnett and Pierce, 2009). The CRB is especially vulnerable to shifts in climate due to the sensitivity of its discharge to precipitation and temperature changes (both of which affect snow accumulation and melt patterns as well as evapotranspiration), and these effects are exacerbated by the semi-arid nature of the basin (Loaiciga, 1996). Given the warming climate and strong reliance of steadily increasing populations on the river and its water storage system, variations in Colorado River flows across the basin are more important now than ever before.

Many studies have examined the effects of climate change on components of the hydrologic budget in the CRB (e.g. Seager et al., 2007; Milly et al., 2005; Christensen et al., 2004; Christensen and Lettenmaier, 2007). Seager et al. (2007) analyzed output from 19 General Circulation Models (GCMs) archived for the Intergovernmental Panel on Climate Change (IPCC). They documented a general trend in almost all the models toward permanently drier conditions in the southwestern U.S. as increased humidity in the tropics induces poleward migration of the subtropical dry zones. The U.S. Climate Change Science Program (USCCSP, 2007) shows, based on results from Milly et al. (2005) (but using a slightly different subset of the 2007 IPCC model runs), that the greatest decreases in runoff by mid-century will range from 10-25 percent, that these changes will occur in the upper and lower Colorado basin, and the Great Basin, and that there is a high degree of agreement among the

models as to the directions of these changes. In contrast, Christensen and Lettenmaier (2007) used statistical downscaling of a slightly different subset of the same GCMs used by Milly et al. (2005) and Seager et al. (2007) to force a physically-based (and more highly spatially resolved) hydrology model over the CRB. They found the mean change in Colorado River discharge, averaged over all GCM A2 emissions scenarios by mid-century, would be a decline of about six percent. Subsequent reanalysis of their results to adjust the hydrology model precipitation forcing to be more consistent with the Milly et al. (2005) results doubles the decline (to about 13 percent), but still shows runoff reductions that are considerably less severe than those projected by Seager et al. (2007). The differences in these estimates of Colorado River discharge to a changing climate have caused considerable concern among western U.S. water managers, and implications go well beyond scientific interest (see e.g. Gertner, 2007). There is, therefore, some urgency in resolving the causes of the differences, to the extent possible.

GCMs are the most appropriate and powerful tool for predicting the effects of climate change; however, formulation of adaptation policies in response to climate change impacts requires information at finer spatial scales than can be represented by GCMs, which typically have grid-cells with dimensions 200-300 km or greater. Thus, although GCMs can provide useful information about possible future changes in atmospheric circulation at the regional (e.g. continental) scale, they do not provide the detail required for regional and national assessments. This is particularly true for heterogeneous regions, where sub-GCM grid-scale variations in topography, vegetation, soils, and coastlines can strongly affect climate. In addition, extreme events, such as heavy precipitation, are often not captured or their intensity is unrealistically low at coarse resolutions.

Regional Climate Models (RCMs), which provide finer spatial detail than GCMs, provide one possible solution to these issues. One shortcoming of RCMs has been that the computational requirements have resulted in an inability to represent the range of inferred future climate conditions in the same way that has been possible through the application of statistical downscaling to the full

suite of IPCC models. The issue is further complicated by the combinatorial problem associated with multiple RCMs (and even specifics of implementation of a given RCM) and multiple GCMs, which would provide the RCM boundary conditions. The North American Regional Climate Change Assessment Program (NARCCAP) has attempted to address this issue by producing multiple RCM simulations over the continental U.S. (Mearns et al., 2009) with different GCM “parents” providing the boundary conditions. Given their relatively high spatial resolution, these simulations should offer more insight into the nature of projections of future climate for the CRB, and in particular, for its runoff. The spatial resolution of the NARCCAP models (typically about 50 km) is much higher than that of the GCMs on which past CRB studies (e.g. Seager et al., 2007; Christensen and Lettenmaier, 2007) have been based. The NARCCAP runs should, therefore, be better able to capture the effects of topographic variations in climate, and hence, should be more useful to address questions regarding the sensitivity of future Colorado River runoff to climate change. We report herein a comparison of Colorado River runoff as inferred from the NARCCAP RCMs and their host GCMs.

2.0 Data description and methods

2.1 RCM output

The general NARCCAP strategy (as in most RCM applications) consists of two phases. In Phase I, six RCMs were forced with global reanalysis from the National Center for Environmental Prediction/Department of Energy (NCEP/DOE) reanalysis (Kanamitsu et al., 2002) as the boundary conditions. Because the reanalysis effectively consists of weather prediction model analysis fields (with “frozen” model versions and analysis systems), it is appropriate to compare the RCM output with observations on a time step basis. In a second phase, GCM output was used to provide boundary conditions for both historic and future climate runs. For the historic run, given the chaotic nature of the atmosphere as represented in the GCM boundary conditions, comparisons with observations is only possible in a statistical context. For future climate runs, no comparison with observations is

possible, of course. We primarily used model output from Phase II, although we made some comparisons with Phase I output as well.

The six RCMs participating in NARCCAP are the Hadley Regional Model 3 (HRM3; Jones et al. 2004), the Regional Climate Model version 3 (RCM3; Giorgi et al., 1993), the Canadian Regional Climate Model (CRCM; Laprise et al., 1998), the NCEP Experimental Climate Prediction Center Regional Spectral Model (ECPC RSM; Juang et al., 1997), the MM5- PSU/NCAR mesoscale model (MM5; Grell et al. 1993), and the Weather Research and Forecasting model (WRF; Skamarock et al., 2005; Leung et al., 2005). The overall design of the NARCCAP experiment is described by Mearns et al. (2009).

In Phase I of NARCCAP, 25-year (1980–2004) RCM simulations were implemented using the NCEP/DOE Reanalysis for boundary conditions. In Phase II, each RCM was nested within at least one GCM at 50-km spatial resolution for the periods 1971-2000 and 2041-2070 (the latter using an SRES A2 global emissions scenario; see Nakićenović and Swart (2000) for details). The RCM-GCM combinations are listed in Table 2.

All of the RCM-based analyses reported here used seasonal and annual means derived from 3-hourly NARCCAP output (Mearns et al., 2007). Five combinations of RCMs and GCMs for Phase II had been archived as of the date of this writing (labeled as “finished” in Table 1). Of those, the MM5/CCSM3 future scenario run had an error, and is being re-run (the current-climate run for this RCM/GCM combination is complete). For the RCM3/CGCM3 and RCM3/GFDL runs, only surface air temperature and precipitation output were archived. Therefore, for evaluation of historical performance, we effectively had access to six RCM/GCM combinations for precipitation (P) and surface air temperature (T), and three combinations for evapotranspiration (ET), runoff (R) and terrestrial storage change (P-ET-R). For the climate change runs, there were five combinations for P and T, and three combinations for ET and R. Because we focus on water budget changes over the CRB,

we only analyzed the three model combinations for which P, ET, and R were all available.

2.2 Host GCMs

For comparison, monthly surface air temperature (T), precipitation (P), evapotranspiration (ET), and runoff (R) for CCSM3, CGCM3, and GFDL CM2.1 were obtained from the World Climate Research Programme's (WCRP's) Coupled Model Intercomparison Project phase 3 (CMIP3) multi-model dataset (e.g. Meehl et al., 2007). The HadCM3 run for NARCCAP was different from that in the CMIP3 archive; therefore, output for this GCM was obtained directly from the NARCCAP team.

2.3 Model evaluation

Land surface variables for the historical period (1970-1999) were taken from the 1/8-degree historical North American Land Data Assimilation System (NLDAS) data set of Maurer et al. (2002). This is the reference dataset for comparisons with the NARCCAP RCMs and the host GCMs. A frequently encountered difficulty in assessing model-predicted land-atmosphere exchanges of moisture and energy is the absence of comprehensive observations to which model predictions can be compared at the spatial and temporal resolutions at which the models operate. The NLDAS data set we used provides both gridded observations (for precipitation and temperature) and model-derived output (e.g., for runoff, snow water equivalent (SWE), and evapotranspiration) for land surface states and fluxes over the conterminous United States and portions of Canada and Mexico. The model-derived output are from the Variable Infiltration Capacity (VIC) land surface model driven by gridded precipitation, temperature and wind time series, as well as downward solar and longwave radiation derived from the daily temperature range and temperature, respectively, following algorithms detailed in Maurer et al (2002). VIC is a macro-scale terrestrial hydrologic model that balances both surface energy and water over each model grid cell (Liang et al., 1994, 1996). The VIC model simulates streamflow, and by closure it is constrained to balance other terms in the land-surface water and energy budgets.

Although direct comparisons of VIC-derived SWE is complicated by point to area comparison issues, when VIC is forced with local meteorology, it has been shown to reproduce observed SWE well (Cherkauer and Lettenmaier, 2003), and it is an attractive surrogate for observations. The Maurer et al. (2002) approach to gridding precipitation and temperature observations preserves observed orographic effects. Furthermore, model-derived variables, like runoff and SWE, are effectively constrained by the fact that model streamflow was calibrated to match observed values. The VIC gridded observations and model-derived variables simulations are described and have been evaluated extensively in publications like Maurer et al (2002) and have previously been used for evaluation of other, less constrained, derived data sets like the NCEP/NCAR reanalysis by Maurer et al. (2001). Similar global derived data sets have been evaluated by Nijssen et al. (2001). Furthermore, the data have been used extensively in widely cited published assessments of climate change impacts on the surface hydrology of the CRB (Christensen et al., 2004; Christensen and Lettenmaier, 2007).

2.4 Methods

We first show that the mean patterns of the driving GCM are reproduced in the RCM simulations for key variables. We then evaluate the finer-scale features that are more resolved by the RCMs than by their host GCMs. The baseline spatial resolution of the RCMs, as run for NARCCAP, is 50 km, whereas the GCMs typically range from 1-4 degrees latitude-longitude. The NLDAS data sets used for evaluation have 1/8-degree spatial resolution, which is considerably finer than either RCMs or GCMs. For comparison, both GCM and RCM output were interpolated to 1/8-degree resolution using an inverse distance squared interpolation, and only points within the CRB were compared. We did not interpolate to coarser spatial resolutions to avoid losing information from the finer resolution. Initially, we evaluated surface air temperature, precipitation, evapotranspiration, runoff, and storage change for the historical period over the CRB. Annual and seasonal changes in the water budget (precipitation, evapotranspiration, and runoff) for the future (2040-2069) period were then compared with the historical period (1970-1999).

3.0 Results: Evaluation for historical period

We first evaluate the historical RCM and GCM simulations through comparisons with NLDAS data (Table 3, Figures 2-11). We focus on surface air temperature (T), precipitation (P), evapotranspiration (ET), runoff (R), and terrestrial storage change (P-ET-R).

3.1 Surface air temperature

In comparisons of 30-year mean T, all the GCMs and RCMs captured obvious T patterns of lower T in the north and higher T in the south (Figure 2). Spatial T patterns of the RCMs and their driving GCMs were highly correlated (greater than 0.89); however, RCMs had a tendency to be warmer in the southern part of the basin and cooler in the northern part of the basin than GCMs (Figure 2, column 3), except for HRM3/HadCM3, which was warmer than HadCM3 over the entire basin (Figure 2, Table 3).

Surface air temperature correlations for the RCMs and NLDAS were much higher than for other variables (Table 3). This implies that regional and global model simulations for T are more reliable than for other variables, which agrees with other studies (Randall et al., 2007; Snyder and Sloan, 2005; Zhang et al., 2009; Leung and Ghan, 1999a; Leung et al., 2003a, 2003b; Plummer et al., 2006). For annual and seasonal T, the spatial correlations between the RCMs and NLDAS were much higher than for GCMs due to the enhanced representation of the land-surface boundary, especially in spring, summer, and fall.

Generally, the RCMs produced better T lapse rates and smaller biases at high elevations than GCMs (Figure 3). The T lapse rate below 2250 m in both GCM and RCM output is well defined (Figure 3). Annual T from GCMs was overestimated above 2250 m and underestimated below. The RCMs have

two obvious T characteristics: (1) they produce more realistic lapse rates than GCMs, especially above 2250 m, (2) RCM performance varied due to different model physics, but the RCMs forced by the same GCMs (WRF/CCSM3 and MM5/CCSM3, CRCM/CGCM3 and RCM3/CGCM3) had similar performance in terms of T (Figure 3). WRF/CCSM3 and MM5/CCSM3 had the best performance above 2250 m.

Seasonally, biases varied for both RCMs and GCMs when averaged over the CRB (Table 3). In the cold season, GCMs had a cold bias and RCMs amplified this cold bias in the forcing data, whereas in the summer GCMs had a warm bias and RCMs had a cold bias (except for HRMs/HADCM3). As a result, RCMs show a colder bias in annual T than GCMs because in GCMs the cold bias in winter is offset by the warm bias in summer (Table 3). The cold season behavior we found coincides with several other studies. Duffy et al. (2006) found that RCMs were also too cold in late winter and spring over the western U.S. MacKay et al. (2003) concluded that annual mean daily temperatures were 1.8 °C colder than observed over the Mackenzie basin. Plummer et al. (2006) found that although CRCM had a warm bias over a large part of the continent, the model had a cold bias between 3° and 4° C over the U.S. Southwest and northern Mexico. Leung et al. (2003a) also found that the WRF simulation was slightly too cool in the southwestern U.S., in spite of a warm bias over the coast and mountains; they associated the cold bias to a longer snow-covered season and larger peak snow water equivalent than was observed.

Biases arise from the host GCM forcings but also from RCM physics. To further explore origins of the biases, we compared the bias from RCM/NCEP and RCM/GCM simulations. We considered the biases of RCM/NCEP simulations to come from errors in model physics ($\text{bias}_{\text{phys}}$) whereas the counterpart for the RCM/GCM simulations represents total bias ($\text{bias}_{\text{total}}$). The absolute of $\text{bias}_{\text{phys}}$ divided by the absolute of $\text{bias}_{\text{total}}$ represents how much physical process errors contribute to the total bias. CRCM had a large cold bias when driven by NCEP (Table 3.1), and the bias was amplified when forced by CGCM3 (Table 3). HRM3 had a large warm bias even when forced by NCEP/DOE (Table

3.1) (the annual bias was much larger than simulations forced by HadCM3). Zhang et al. (2009) also found that HRM3 had a warmer bias compared to WRF, even using the same NCEP/DOE forcing over the U.S. Pacific Northwest. The contribution of physical process errors to total bias was 40% and 60% for CRCM and HRM3, respectively. However, WRF, MM5, and RCM3 biases came mostly from their GCMs, with the contribution from physical process errors being 5% or less. For example, RCM3/GFDL had the largest cold bias relative to other RCMs, which was not present when RCM3 was forced by NCEP/DOE (Table 3.1). This indicates that the bias largely came from the GFDL GCM forcing. In general, our analysis suggests that depending on the GCM, the bias not only relates to the host GCM, but also to model physical processes, and that the relative contributions vary considerably among the GCM/RCM combinations.

3.2 Precipitation

The seasonal cycle of precipitation was not as well represented as temperature by either GCMs or RCMs (Table 3). This is consistent with many previous studies (Randall et al., 2007; Snyder and Sloan, 2005; Zhang et al., 2009; Leung et al., 2003a, 2003b; Plummer et al., 2006).

Spatial correlation of annual precipitation between GCMs and NLDAS ranges from 0.22 to 0.40. None of the four GCMs was able to capture the higher annual precipitation over the mountainous part of the CRB, and some were unable to represent dry conditions in the lowlands because of their coarse spatial resolution (Figure 5). In winter, precipitation had mostly negative spatial correlations with NLDAS (Table 3). Figure 5 shows that precipitation in winter mostly occurred at 1800 m for GCMs, not above 2500 m as it occurred in NLDAS, which again is due to the coarse GCM resolution that does not distinguish the considerable topographic changes in the CRB. There is not enough dynamical uplift in GCMs because of their smoothed topography (Leung and Ghan, 1999a). Castro et al. (2007) also states that GCMs cannot properly represent the diurnal cycle that strongly depends on terrain-induced convection; this is the most important value-added component of the enhanced

representation of the land-surface boundary of the RCMs. In summer, GCMs had better lapse rates than winter, so unrealistic annual lapse rates for GCMs were largely from winter differences (Figure 5).

In contrast to GCMs, the RCMs have enhanced variation in precipitation with elevation because of their finer topography (Figure 5). Spatial correlations of annual precipitation between the RCMs and NLDAS ranged from 0.60 to 0.73 (Table 3) (summer correlations were smaller, not surprisingly as even RCMs were unable to resolve the small scale processes that dominate precipitation during the warm season). Improvements in RCMs (relative to their host GCMs) in winter and spring are especially apparent (Table 3). The RCM simulations were closer to NLDAS than GCMs, except for over-simulations in HRM3/HadCM3 and RCM3/GFDL (Figure 5). WRF/CCSM3 and CRCM/CGCM3 were biased low at high elevations despite improvements relative to their host GCMs (Figure 5).

Consistent with their host GCMs, all RCMs produced more precipitation in winter and less (except HRM3/HadCM3 and RCM3/GFDL) in summer, hence the annual values and correlations reflect some compensation of these differences (Table 3). A robust amplification of cold season precipitation was also found by Wang et al. (2009) based on NARCCAP Phase I analysis, Leung et al. (2003a, b) based on MM5 simulations, and Giorgi et al. (1992) based on RCM3 simulations. Summer precipitation simulations had a larger inter-model spread than in other seasons, which is also suggested by the lower spatial correlations noted above. Basic convective research (e.g., Kain and Fritsch, 1990) indicate that warm season precipitation is especially sensitive to differing representations of sub-grid convection. Previous studies (Gochis et al., 2002; Liang et al., 2007) also found that RCM simulations of precipitation in the North American Monsoon region (which includes the southern part of the CRB) were quite sensitive to the choice of the convective parameterization. The NARCCAP models use different convective and microphysical parameterizations. In this context, the differences in summer precipitation are not surprising. Furthermore, given the sub-grid nature of convective precipitation

(and to a lesser extent, representations of cold-season processes), the 50-km NARCCAP resolution still has limitations in resolving precipitation in topographically complex regions like the CRB, notwithstanding that the spatial resolution is much finer than that of the GCMs.

Unlike air temperature, the RCMs differed in how well they simulate precipitation even when forced by the same GCMs. For example, WRF/CCSM3 and MM5/CCSM3 had similar precipitation simulations at low elevations, but MM5 simulated precipitation better than WRF at high elevations. This suggests differences in physical processes related to topography. Differences due to how physical processes were simulated are also apparent when host GCMs were coupled with different RCMs. For example, CRCM/CGCM3 simulated precipitation better than RCM3/CGCM3. CRCM/CGCM3 had the smallest biases among the RCMs in both annual mean and monthly averages (Table 3), whereas RCM3/CGCM3 overestimated precipitation, especially in winter. The wetter bias by RCM3/CGCM3 was partly from model physics parameterizations. RCM3 had wet biases with GFDL too, greatly overestimating precipitation in winter and at high elevations in summer (Figure 5). Because the only difference between RCM3/CGCM3 and RCM3/GFDL was their forcings, this larger bias is also attributable to the host GCMs.

3.3 Evapotranspiration

Evapotranspiration (ET) was archived by NARCCAP for three RCM/GCM combinations: CRCM/CGCM3 (CRCM for short in the following), HRM3/HadCM3 (HRM3), and WRF/CCSM3 (WRF). The three GCMs did not have much spatial variation and did not capture ET distributions at high elevations well, especially CCSM3 (Figure 6, column II). Not surprisingly, the RCMs better resolved inferred regional variations (Figure 6, column I). The RCMs had higher spatial correlation with NLDAS and also captured ET magnitude better than GCMs, especially in summer (Table 3).

Performance varied for each RCM. WRF matched NLDAS better than the other two RCMs, except for

slight underestimations below 1800 m, which occurred mostly in summer. CRCM had almost the same performance as its host CGCM3, which underestimated annual ET at high elevations and overestimated ET at low elevations. HRM3, consistent with its host HadCM3, overestimated annual ET, especially in high elevations (Table 3, Figure 7).

Because ET is limited by moisture availability over much of the basin, the ET lapse curve follows precipitation patterns to some extent (compare Figures 5 and 6), especially below 2600 m. Generally, the RCMs tended to overestimate ET in winter and underestimate ET in summer, especially for elevations below 2000 m, which is consistent with the modeled precipitation patterns in Figure 5.

3.4. Runoff

As Figure 8 shows in the 30-year mean spatial distribution of runoff over the CRB, most of the runoff comes from the mountains, which cover a small portion of the total basin area in the north. The RCMs better reproduced the basic spatial characteristics of the surface hydrology and topographically induced characteristics of runoff over the CRB than the GCMs as also found in earlier studies (e.g., Giorgi et al. 1994). The RCMs generally had much higher correlations with NLDAS runoff than their host GCMs, especially HRM3/HadCM3 and CRCM/CGCM3 (Table 3). Nonetheless, runoff correlations were lower than for P and ET. In WRF the spatial correlation was low, although it captured the runoff magnitude well. The GCMs generally overestimated runoff in winter, whereas RCM runoff was closer in magnitude to NLDAS than GCMs, especially in winter (Table 3). This is because in the CRB, runoff is driven by springtime snow melt, which in turn results from winter snow accumulation. As noted in section 3.1, RCMs generally had colder temperatures than GCMs; these colder temperatures promote winter snow accumulation at high elevations, where a large portion of the CRB's runoff is generated (Barnett et al., 2005; Barnett and Pierce, 2009; Cayan et al., 2010).

The maximum runoff for the RCMs occurred in spring, not spring-summer as in NLDAS (Table 3),

and runoff in spring was mostly overestimated, especially in HRM3. This mismatch is linked with underestimated runoff in summer, mainly because of the underestimation of precipitation and the overestimation of snowmelt in spring. This suggests that spring runoff is quite sensitive to the model treatment of snow cover relative to temperature, as also indicated by Plummer et al. (2006) and MacKay et al. (2003).

Similar to P and ET, the RCMs captured runoff variations with elevation better than GCMs (Figure 9). The NLDAS distribution implied that most of the CRB's runoff comes from areas above 2250 m, and decreases sharply at lower elevations. For the three host GCMs, runoff was mainly from elevations that range from 2000 m to 2400 m, especially CCSM3 and CGCM3 in winter, and not from the highest elevations as implied by NLDAS. The large runoff at mid-elevation in winter was mostly consistent with precipitation. Commonly, in winter, precipitation falls as snow rather than rain due to temperatures below freezing. But snow cover in CCSM3 and CGCM3 was located at lower elevations than in other models (Figure 10) where temperature was near freezing in the diurnal cycle (Figure 3). The accumulation of low-elevation snow cover and the overall higher temperatures of CCSM3 and CGCM3 resulted in increased runoff. Furthermore, snowfall at low elevations is mostly related to the GCM's weak uplift due to the smoothed topography and model physics in the cold season. Also, it is notable that all GCMs and RCMs underestimated runoff production in summer (Figure 9) and fall (not shown).

Of the models considered here, HRM3/HadCM3 simulated the most realistic annual runoff. It produced large runoff from high elevations in summer; although not as large as NLDAS (none of the RCMs reproduced the large observed summertime runoff values). WRF/CCSM3 overestimated winter runoff especially at elevations below 2400 m, underestimated snow water equivalent (SWE) in winter, and missed most summer runoff as a result of the underestimation of high-elevation precipitation (section 3.2; Table 3). It therefore had significant negative bias in annual runoff for elevations above 2250 m. CRCM/CGCM3 had slight improvement relative to its host CGCM3 at high elevations but

missed the summer runoff because of underestimation of high-elevation precipitation.

3.5. Terrestrial storage change

We calculated the change in terrestrial storage as $P-ET-R$, an index of water budget closure. As mentioned previously, we used an off-line VIC run as the source of surrogates of NLDAS runoff and ET, which we combined with gridded precipitation observations to compute NLDAS storage change. In all RCMs, water balance (change in storage on an annual basis averaged over the historical period) approached zero (Table 3), which is essentially the same as NLDAS. Although annual mean $P-ET-R$ was zero, these values vary for each season. In winter and fall, $P-ET-R$ was positive, especially above 2250 m, and in summer and spring, it was negative (Table 3), especially at high elevations (Figure 11); however, none of the GCMs had summer drying to the extent inferred from NLDAS. The RCMs showed conditions that are slightly drier than GCMs in spring and summer, although not as much as NLDAS. Generally, $P-ET-R$ was opposite of the runoff pattern (Figure 11).

4.0 Results and discussion: Climate change impacts

To evaluate climate change and related impacts on water availability, we focus on temperature and runoff change as well as snow cover and precipitation between future (2040-2069) and historical (1970-1999) simulations for three RCM/GCM combinations: CRCM/CGCM3 (CRCM for short in this section), HRM3/HadCM3 (HRM3), and WRF/CCSM3 (WRF). We selected these GCM/RCM combinations because they are the only ones for which all of the variables of interest were archived.

4.1 Temperature changes

First, we examine climate change-induced differences in temperature over the CRB (Figure 12). RCMs projected warming signals that are consistent with their host GCMs. All RCMs and GCMs projected more warming in the north than south (Figure 12, left) and more warming in the warm

season than in the cold season (right). The magnitude of changes between RCMs and GCMs, however, differed, depending on the season. In the cold season, the RCMs projected less warming than GCMs (Figure 12, right). However, in the warm season, two RCMs (CRCM and HRM3) projected stronger warming than their host GCMs. WRF projected less warming than CCSM3. In the CRB, snowmelt is the source of runoff, and for this reason, warming in the cold season has a very strong influence on water availability. It is worth noting that effects of increased atmospheric CO₂ on the surface air temperature from the RCMs show strong elevation dependencies, consistent with Giorgi et al. (1997), Leung and Ghan (1999b), and Kim et al. (2002).

4.2 Climate change impacts on water availability and related variables

Generally, annual runoff changes for the RCMs were consistent with their host GCMs (see ANN, Figure 13). CCSM3 and CGCM3 projected decreases in annual runoff, whereas HadCM3 projected slight increases. Consistent with their host GCMs, CRCM and WRF had decreasing runoff, with the same pattern but different magnitudes (Figure 13). HRM3 had a slight increase in annual runoff, consistent with HadCM3. Runoff changes for RCMs and GCMs mostly occurred in winter (DJF), spring (MAM), and summer (JJA) (Figure 13, right). These results from runoff being impacted by the combination of three factors: snow cover change in winter, temperature change in spring, and precipitation change in all seasons. In summer, with temperatures considerably above freezing, the changes in runoff were mostly consistent with those of precipitation. In winter and spring, however, runoff change was complicated due to snowmelt. We highlight changes in winter, spring, and summer to show how RCMs and GCMs differ in how they represent the susceptibility of headwater streams to climate change.

4.2.1 Winter

In winter, all RCMs and GCMs projected runoff increases except for WRF (Figure 13, right). HRM3 projected larger increases than its host, HadCM3, whereas CRCM projected smaller increases than its host CGCM3. Runoff changes primarily tracked precipitation and snow cover changes (Figures 13, 14,

and 15). The increase in CCSM3 runoff closely tracked the trend in snow cover (Figures 13 and 15). Different temperature simulations resulted in different snow cover in RCMs and GCMs. In the upper basin, most areas of CCSM3 snow cover were located near the freezing level, which is lower than other GCMs and RCMs (Figure 9). Lower elevation snow was more susceptible to melting in response to varying temperatures; this, in turn, led to larger runoff. WRF projected decreased runoff as a result of the combination of no precipitation change (Table 4; Figure 5) and increased evapotranspiration (Table 5; Figure 7) due to increased temperature (Table 8; Figure 12). Generally, smaller winter precipitation increases (CRCM/CGCM3 and HRM3/HadCM3, Table 4) and reduced snowmelt (WRF/CCSM3, Table 7) were the main reasons for smaller winter runoff increases in the RCMs than in the GCMs (Figure 13).

4.2.2 Spring

The most significant change and differences in changes across models occurred in spring (Figure 13, right). In the western U.S., the runoff-change signal tracks temperature and snow cover change. GCM runoff decreased dramatically in CCSM3 and CGCM3 due to reduced snowmelt (Figure 13 and 15); whereas, in HadCM3 runoff slightly increased. In contrast, the RCMs predicted smaller runoff decreases or larger increases than their host GCMs, especially for WRF (Figure 13). The lower-elevation snow cover (Figure 10) and larger warming (Figure 12) caused larger reductions in snow cover for GCMs than for RCMs (Figure 15). Larger snowmelt leads to lower albedo. The reduced albedo absorbs more energy and generates positive feedback for more warming and increased snowmelt as a result of enhanced warming. As a result, GCMs projected larger temperature increases than the RCMs in spring (Figure 12); temperature differences are especially notable between WRF and its host CCSM3. WRF projected 2.2 °C increases over the CRB, while CCSM3 projected 3.0 °C increases. Similar to its response in winter, HRM3 projected larger runoff increases in spring at high elevations. In contrast, its host GCM (HadCM3) predicted almost no change in spring. Leung and Ghan (1999b) also found a negative signal over the CRB (see their Figure 7), although over the Pacific Northwest they concluded the opposite in that the RCM warming signal is stronger than the

CCSM3 signal during winter in most areas of the Pacific Northwest. This indicates that climate change susceptibility as simulated by the RCMs as contrasted with GCMs depends on the particulars of the region being investigated.

The surface temperature, snow cover, and runoff change signals were strongly elevation dependent. Furthermore, most reductions of snow cover were near the snow line in the control simulation, which is consistent with Giorgi et al. (1997), Leung and Ghan (1999b), and Kim et al. (2002). Leung and Ghan (1999b) and Kim et al. (2002) attributed runoff change in spring to higher freezing levels in the future climate, and Kim et al. (2002) stated that the warming signal between 1000 and 2000 m is larger than areas over 2000 m in the Western U.S. For the CRB, the snow line is often above 2000 m (Figure 10). In our study, all the RCMs and HadCM3 agreed with NLDAS surrogates for SWE as to how snow accumulation changes with elevation, although they underestimated snow amounts. For CCSM3, however, the snow amount was not only under-predicted, but the snow line was predicted to be much lower than NLDAS (Figure 10). Most of the snow was located between 1700-2400 m in CCSM3, which was lower than the location of snow in WRF. As freezing levels become higher in the future, large amounts of snow from below 2000 m melted in CCSM3 but not in the RCMs. Therefore, since CCSM3 had a lower snow line, snow was easier to melt in CCSM3 than in other models. The reduced albedo, due to increased snowmelt, led to greater absorption of radiation, which raised surface temperatures. Raised temperatures accelerated snowmelt further and caused significant changes in runoff (Figure 13; Table 6) and temperature (Figure 15; Table 8). Thus, consistent with previous studies, the elevation-dependent runoff and temperature signal is mainly related to reduce winter snowfall and spring-summer snow cover in high altitudes in the altered climate. The snow-albedo feedback plays an important role in determining the climate change signal.

4.2.3 Summer

Runoff change differences between RCMs and GCMs also occurred in summer (although they contribute less to annual flow changes). All RCMs projected decreases in summer runoff, whereas

their host GCMs projected no change for CGCM3 and HadCM3 and increases for CCSM3 (Figure 13). The runoff change difference between the RCMs and GCMs in summer resulted mostly from differences in precipitation changes; the RCMs projected greater decreases than the GCMs in summer (Figure 14; Table 4), in agreement with Leung and Ghan (1999b) over the CRB. Runoff changes at low elevations were similar to the host GCMs, but differed at high elevations, which we discuss further in section 4.3.

4.3 Climate change impacts at high elevations

As mentioned above, climate change is highly elevation-dependent over the CRB. Much of the runoff comes from areas above 2250 m (Figure 9; Hoerling et al., 2009; Franz et al., 2003; Cayan et al., 2001). Areas with elevations higher than 2250 m occupy about 22% of the basin's area (Figure 1c). Table 6 lists annual and seasonal runoff changes above this threshold. Differences between the RCMs and GCMs were most prominent in winter, spring, and summer. In winter, all RCMs and GCMs except WRF showed increases in runoff. Two RCMs (CRCM and HRM3) projected larger increases than their host GCMs (CGCM3 and HadCM3 respectively). In spring, two RCMs projected smaller decreases than their host GCMs, specifically -19% for WRF and CRCM, compared to -50% and -27% for CCSM3 and CGCM3, respectively, whereas HRM3 and its host HadCM3 projected increases in spring, with HRM3 projecting a smaller increase than HadCM3. This result agrees with Govindasamy et al. (2003) and Sushama et al. (2006) who mention the importance of regional scale differences in snowpack changes between the high-resolution simulations relative to the low-resolution of GCMs, due to better representation of topography at high resolutions. In summer, CCSM3 projected increases in runoff; however, WRF projected no change. CGCM3 projected increases; however, CRCM projected decreases. HadCM3 projected slight decreases; however, HRM3 projected larger decreases than HadCM3 (Table 6).

Consistent with the spatial average over the entire basin, annual runoff change for all the RCMs and

GCMs was controlled by the change signal in spring (Figure 13; Table 6). Runoff change in spring was from changes in snow water equivalent (see SWE, Table 7), which was strongly related to temperature change (Table 8; Figure 13). All RCMs and GCMs projected that, as temperatures rise, snow reductions were greater in spring than in winter. The spring trend was more influential than in winter because, while the change magnitudes were similar, the atmosphere's variability was smaller in the spring than in winter (Cayan et al., 2001). Recent studies have documented that observed recent warming caused by earlier runoff during the spring snowmelt period was most pronounced in the mountains of the western states, where snowpack temperatures usually are not far below freezing (Cayan et al., 2001; Stewart et al., 2005; Mote, 2006; Clow et al., 2010). Cayan et al. (2001) also noted that even the mountains of Colorado, with their high elevations and cold snowpacks, are experiencing substantial shifts in the timing of snowmelt and its runoff toward earlier in the year. They also state that increasing springtime air temperatures and declining SWE could account for a large portion of the variance in snowmelt timing.

Annual surface air temperature predicted by the RCMs is 2-7°C lower than that predicted by GCMs above 2250 m (Table 8). The RCMs predicted smaller temperature increases in spring than GCMs (Table 8). As a result, RCMs projected smaller snow reduction percentages than their host GCMs. In spring, SWE reductions were -41%, -33%, and -32% for WRF, CRCM, and HRM3, respectively, compared to -73% and -50% for CCSM3 and CGCM3. Higher reduction percentages for the GCMs were likely because of the higher temperature projections for GCMs at high elevations where snow accumulation and melting occurs (Table 6-8; Figure 15). Generally, changes in snow distribution coincide with temperature change. Our results indicate that the RCMs and GCMs both projected that the headwater streams will be affected by a warming climate; however, they are much less susceptible in the RCMs than in the GCMs.

5.0 Value added from RCM simulations

As mentioned above, the value of RCMs lies, not surprisingly, in their ability to add meaningful

spatiotemporal detail to global-scale information with more highly resolved representations of surface forcing (e.g. topography and snow cover). Additionally, their superior formulations of model physics processes can contribute to improved skill in downscaled results beyond just changes in surface forcing (Duffy et al., 2006; Han and Roads, 2004). In our results, RCM simulations at high elevations were more reliable compared to GCMs because of their finer resolution, but also because they had stronger upward lift triggered by their finer distribution in topography. In the CRB, stronger lift raises air parcels higher and results in higher snow lines in RCMs than in GCMs. As a result, runoff change in the CRB was less susceptible to climate change in RCMs than in GCMs. However, one can question the fairness of comparing at the finer resolution with elevation because GCMs inherently were constrained to have a smoother representation of topography than RCMs, especially at the highest elevations. To address this fairness, we aggregated the RCMs and GCMs to 2.5-degree spatial resolution (each GCM has a different resolution). This was close to the mean spatial resolution of the GCMs (Figure 16). When spatially aggregated, there generally was still more variation in grid cells between RCMs than GCMs, especially during the spring, which suggests that the differences we observe in the RCMs are not related only to their higher spatial resolution.

Déqué et al. (2005) used the intermodel standard deviation as a measure of the dispersion of GCMs and RCMs about their centroid. We performed a similar calculation, results of which are shown in Table 9. The results show that the GCM projection spread is larger than for the RCMs not only for annual temperature, but also for annual precipitation and annual runoff. The seasonal spread is smaller for RCMs than GCMs in winter for temperature/precipitation and in spring for runoff. In this sense, there is less intermodel uncertainty in the RCM results relative to those from the GCMs.

6.0 Conclusions

Performance of the Regional Climate Model (RCM) historical simulations forced by four GCMs run for the North American Regional Climate Change Assessment Program (NARCCAP) Phase II was

analyzed in comparison to the 1/8-degree historical North American Land Data Assimilation System (NLDAS) data set over the Colorado River Basin (CRB). Future (2040-2069) simulations over the CRB using the A2 SRES emission scenario were then compared to historical runs (1970-1999) for the RCMs relative to their host GCMs. Through these comparisons we found that although the RCMs and their host GCMs often have similar patterns for surface temperature, precipitation, and evapotranspiration, in the CRB there are spatial and seasonal differences that result in runoff values in the RCMs being less susceptible to a warming climate than their host GCMs. Our key findings are:

(1) The RCMs capture the primary features of the observed land–surface water budget and surface temperature better than their host GCMs in part because of their ability to better represent strong upward lift in topographically complex regions. Although the RCMs do not have significantly improved simulations of precipitation relative to the GCMs, their ability to better represent surface temperature in mountainous regions has important effects on simulations of evapotranspiration, snowpack, and runoff. This improved skill in simulating temperature is important for detecting climate change signals in the topographically diverse CRB.

(2) Runoff generation and change in the CRB is highly elevation dependent. Headwater streams contribute most of the downstream flow, and annual runoff change signals are primarily controlled by changes in the snowmelt period. Therefore the response of cold-season temperatures in headwater streams is key to determining the basin’s susceptibility to a warming climate. In the CRB, runoff changes are generally impacted by the combination of three main factors: snow cover in winter, temperature change in spring, and precipitation change in summer.

(3) The RCMs have similar annual climate change signals (although with slightly smaller magnitudes) to their host GCMs. All RCMs and GCMs had larger warming in the north than in the south and more warming in the warm season than in the cold season; however, the magnitude of these changes differ between RCMs and GCMs, and is notably different depending on the season. Compared to the host

GCMs, the RCMs project larger decreases in precipitation and evapotranspiration in summer, which translated to larger reductions in summer runoff in the RCMs. Alternatively, in the cold season, RCMs project less warming than GCMs. Therefore, although both RCMs and GCMs project decreases over the CRB, the RCMs projected less warming in the spring and thus have smaller decreases in runoff in the spring (arising from smaller temperature changes and better topographic resolution), which results in smaller decreases in annual runoff as compared with the GCMs. Thus, surface air temperature, runoff, and snow water equivalent changes at high elevation all indicate that headwater streams are less susceptible to a warming climate in the RCM climate change simulations than in GCM simulations.

(4) Climate change susceptibility as simulated by the RCMs as contrasted with GCMs depends on the particulars of the region being investigated. Specifically, our results indicate smaller runoff differences in the future in RCMs than in GCMs, primarily because GCMs do not adequately simulate higher elevations where temperature changes have less affect on snow cover (where temperatures are still cold enough to retain snow). In regions where runoff originates in lower elevations, results may differ (e.g. Leung and Ghan, 1999b; Kim et al., 2002).

It should also be noted that although the NARCCAP RCMs captured the primary features of observations and more closely reproduced the NLDAS estimates than do the host GCMs, the 50-km grid resolution may still not be fine enough to resolve orographic effects in parts of the domain. As shown by Ghan et al. (1997, 2006) sub-grid variability in summertime precipitation can have substantial effects on surface hydrology, and sub-grid variations in vegetation and soil properties also increase surface runoff and reduce evapotranspiration. Furthermore, there remain a number of other uncertainties associated with RCM climate change scenarios. First, the climate change signal for RCMs is dependent on the circulation from the driving GCM. Errors in the GCM response to global emissions forcing will be transferred to the RCMs. We have noted several situations where the RCMs clearly have inherited bias from the parent forcing. Second, the models differ in their ability to project

climate change due to different physics, yet because only a limited number of GCM/RCM combinations have been completed and archived to date, understanding these physics is challenging. As Duffy et al. (2006) pointed out, RCM estimates of water content and projections of change in water content vary. Therefore, further synthesis investigations linking the atmosphere and terrestrial components of the water cycle that are based on more RCMs are necessary.

Acknowledgements:

We thank NARCCAP for providing the data used. NARCCAP is funded by the National Science Foundation (NSF), the U.S. Department of Energy (DoE), the National Oceanic and Atmospheric Administration (NOAA), and the U.S. Environmental Protection Agency Office of Research and Development (EPA). We acknowledge the contributing NARCCAP modeling groups, the Program for Climate Model Diagnosis and Intercomparison (PCMDI) and the WCRP Working Group on Coupled Modeling (WGCM) for their roles in making available the GCM data. Support of this data set is provided by the Office of Science, U.S. Department of Energy. This work was supported by a DoE Grant DE-FG02-08ER64589.

References:

- Barnett, T., J. C. Adam, and D. P. Lettenmaier, 2005: Potential impacts of a warming climate on water availability in snow-dominated regions. *Nature*, 438, 303-309, doi:10.1038/nature04141.
- Barnett T. and David W. Pierce, 2009: Sustainable water deliveries from the Colorado River in a changing climate. *PNAS*, 106(18), 7334–7338. [available online: <http://www.ncbi.nlm.nih.gov/pmc/articles/PMC2678624/pdf/zpq7334.pdf>]
- Castro, C. L., R. A. Pielke Sr., and J. O. Adegoke, 2007: Investigation of the summer climate of the contiguous United States and Mexico using the Regional Atmospheric Modeling System (RAMS). Part I: Model climatology (1950–2002). *J. Climate*, 20, 89–110.
- Cayan D. R., Michael D. Dettinger, Susan A. Kammerdiener, Joseph M. Caprio, David H. Peterson, 2001: Changes in the Onset of Spring in the Western United States. *Bulletin of the American Meteorological Society*, 82, 399-415.
- Cherkauer, K. A., and D. P. Lettenmaier, 2003: Simulation of spatial variability in snow and frozen soil, *J. Geophys. Res.*, 108(D22), 8858, doi:10.1029/2003JD003575.
- Christensen, N.S., Wood, A.W., Voisin, N., Lettenmaier, D.P. and R.N. Palmer, 2004: Effects of Climate Change on the Hydrology and Water Resources of the Colorado River Basin, *Climatic Change*, 62(1-3), 337-363.
- Christensen N. and D.P. Lettenmaier, 2007: A multimodel ensemble approach to assessment of climate change impacts on the hydrology and water resources of the Colorado River Basin, *Hydrol. Earth System Sci.* 11, 1417-1434.
- Clow D. W., 2010: Changes in the Timing of Snowmelt and Streamflow in Colorado: A Response to Recent Warming. *Journal of Climate*, 23, 2293-2306.
- Déqué M., R. G. Jones, M. Wild, F. Giorgi, J. H. Christensen, D. C. Hassell, P. L. Vidale, B. Rockel, D. Jacob, E. Kjellstro, M. de. Castro, F. Kucharski, B. van den Hurk, 2005: Global high resolution versus Limited Area Model climate change projections over Europe: quantifying confidence level from PRUDENCE results. *Climate Dynamic*, 25, 653-670.
- Duffy P. B., R. W. Arritt, J. Coquard, W. Gutowski, J. Han, J. Iorio, J. Kim, L.-R. Leung, J. Roads, E.

- Zeledon, 2006: Simulations of Present and Future Climates in the Western United States with Four Nested Regional Climate Models, *Journal of Climate*, 19, 873-895.
- Franz K. J., Holly C. Hartmann, Soroosh Sorooshian, Roger Bales, 2003: Verification of National Weather Service Ensemble Streamflow Predictions for Water Supply Forecasting in the Colorado River Basin. *Journal of Hydrometeorology*, 4, 1105-1118.
- Gertner, J., 2007. The future is drying up, *New York Times Magazine*, Oct. 21, 2007 (www.nytimes.com/2007/10/21/magazine/21water-t.html)
- Ghan, S. J., J. C. Liljegren, W. J. Shaw, J. H. Hubbe, J. C. Doran, 1997: Influence of Subgrid Variability on Surface Hydrology. *J. Climate*, 10, 3157–3166.
- Ghan, S. J., T. Shippert, J. Fox, 2006: Physically Based Global Downscaling: Regional Evaluation. *J. Climate*, 19, 429–445. doi: 10.1175/JCLI3622.1
- Giorgi F., G. T. Bates, S. J. Nieman, 1992: Simulation of the Arid Climate of the Southern Great Basin Using a Regional Climate Model, *Bulletin of the American Meteorological Society*, 73, 1807-1822.
- Giorgi, F., M.R. Marinucci, and G.T. Bates, 1993: Development of a second generation regional climate model (RegCM2) I: Boundary layer and radiative transfer processes. *Mon. Wea. Rev.*, 121, 2794-2813.
- Giorgi, F., S.W. Hostetler and C. Shields Brodeur, 1994: Analysis of the surface hydrology in a regional climate model. *QJRMS*, V120, 161-184.
- Giorgi, F., J. W. Hurrell, M. R. Marinucci, M. Beniston, 1997: Elevation Dependency of the Surface Climate Change Signal: A Model Study. *J. Climate*, 10, 288–296.
- Gochis D. J., W. J. Shuttleworth, Z.-L. Yang, 2002: Sensitivity of the modeled North American Monsoon regional climate to convective parameterization. *Mon. Wea. Rev.*, 130, 1282–1298.
- Govindasamy B., P. B. Duffy, and J. Coquard, 2003: High-resolution simulations of global climate, part 2: effects of increased greenhouse cases. *Climate Dynamics*, 21, 391–404, doi: 10.1007/s00382-003-0340-6.
- Grell, G., J. Dudhia, and D. R. Stauffer, 1993: A description of the fifth-generation Penn State/NCAR

- mesoscale model (MM5). NCAR Tech. Note NCAR/TN-398 1 IA, National Center for Atmospheric Research, 107 pp.
- Han, J., and J. Roads, 2004: U.S. climate sensitivity simulated with the NCEP regional spectral model. *Climate Change*, 62, 115–154, doi:10.1023/B:CLIM.0000013675.66917.15.
- Hoerling M., Dennis Lettenmaier, Dan Cayan, and Brad Udall, 2009: Reconciling Projections of Colorado River Streamflow, *Southwest Hydrology*, 20, 29-31.
- Jones, R. G., M. Noguer, D. C. Hassel, D. Hudson, S. S. Wilson, G. J. Jenkins, and J. F. B. Mitchell, 2004: Generating high resolution climate change scenarios using PRECIS. Met Office Hadley Centre, 40 pp.
- Juang, H.-M. H., S.-Y. Hong and M. Kanamitsu, 1997: The NCEP regional spectral model: an update. *Bulletin Amer. Meteor. Soc.*, 78, 2125-2143
- Kain, J. S., and M. Fritsch, 1990: A one-dimensional entraining/detraining plume model and its application in convective parameterization. *J. Atmos. Sci.*, 47, 2784–2802.
- Kanamitsu M., W. Ebisuzaki, J. Woollen, S. Yang, J. J. Hnilo, M. Fiorino, and G. L. Potter, 2002: NCEP–DOE AMIP-II Reanalysis (R-2). *Bull. Amer. Meteor. Soc.*, 83, 1631–1643.
- Kim, J., 2001: A nested modeling study of elevation-dependent climate change signals in California induced by increased atmospheric CO₂. *Geophys. Res. Lett.*, 28, 2951–2954.
- Kim, J., Kim, T., Arritt, R. W., and Miller, N. L., 2002: Impacts of increased atmospheric CO₂ on the hydroclimate of the western United States. *J. Climate*, 15, 1926–1942.
- Laprise, R., D. Caya, M. Giguère, G. Bergeron, H. Côté, J.-P. Blanchet, G. J. Boer, and N. A. McFarlane, 1998: Climate of Western Canada under current and enhanced greenhouse gas concentration as simulated by the Canadian Regional Climate Model, *Atmos.-Ocean*, 36(2), 119-167.
- Leung L. Ruby. and S. J. Ghan, 1999a: Pacific Northwest Climate Sensitivity Simulated by a Regional Climate Model Driven by a GCM. Part I: Control Simulations. *J. of Climate*, 12, 2010-2030
- Leung L. Ruby. and S. J. Ghan, 1999b: Pacific Northwest Climate Sensitivity Simulated by a Regional Climate Model Driven by a GCM. Part II: 23CO₂ Simulations. *J. of Climate*, 12, 2031-2053.

- Leung L. Ruby, Yun Qian, Xindi Bian, 2003a: Hydroclimate of the Western United States Based on Observations and Regional Climate Simulation of 1981–2000. Part I: Seasonal Statistics. *Journal of Climate*, 16, 1892-1911.
- Leung L. Ruby, Yun Qian, Jongil Han, John O. Roads, 2003b: Intercomparison of Global Reanalyses and Regional Simulations of Cold Season Water Budgets in the Western United States, *Journal of Hydrometeorology*, 4, 1067-1087.
- Leung, L.Ruby, J. Done, J. Dudhia, T. Henderson, M. Vertenstein, and B. Kuo, 2005: Preliminary results of WRF for regional climate simulations. Presented at Workshop Research Needs and Directions of Regional Climate Modeling Using WRF and CCSM, March 22-23, 2005, Boulder, CO. (Available at:http://box.mmm.ucar.edu/events/rcm05/presentations/leung_rcm_workshop.pdf)
- Liang, X., D. P. Lettenmaier, E. F. Wood, and S. J. Burges, 1994:A simple hydrologically based model of land surface water and energy fluxes for general circulation models. *J. Geophys. Res.*, 99 (D7), 14 415–14 428.
- Liang, X., E. F. Wood, and D. P. Lettenmaier, 1996: Surface soil moisture parameterization of the VIC-2L model: Evaluation and modifications. *Global Planet Change*, 13, 195–206.
- Liang X., M. Xu, K. E. Kunkel, G. A. Grell, J. S. Kain, 2007: Regional Climate Model simulation of U.S.–Mexico summer precipitation using the optimal ensemble of two cumulus parameterizations. *J. Climate*, 20, 5201–5207. doi: 10.1175/JCLI4306.1.
- Loaiciga, H. A., Valdes, J. B., Vogel, R., Garvey, J., and Schwarz, H., 1996: Global warming and the hydrologic cycle, *J. Hydrol.*, 174, 83–127.
- Maurer E. P., G. M. O’Donnell, D. P. Lettenmaier, and J. O. Roads, 2001: Evaluation of the land surface water budget in NCEP/NCAR and NCEP/DOE reanalyses using an off-line hydrologic model. *J. Geophys. Res.*, 106 (D16), 17 841–17 862.
- Maurer E. P., A.W. Wood, J.C. Adam, D.P. Lettenmaier, and B. Nijssen, 2002: A Long-Term Hydrologically-Based Data Set of Land Surface Fluxes and States for the Conterminous United States, *J. Climate* 15, 3237-3251

- MacKay M. D., F. Seglenieks, D. Verseghy, E. D. Soulis, K. R. Snelgrove, A. Walker, K. Szeto, 2003: Modeling Mackenzie Basin Surface Water Balance during CAGES with the Canadian Regional Climate Model, *Journal of Hydrometeorology*, 4, 748-767.
- Mearns, L.O., et al., 2007, updated 2011. The North American Regional Climate Change Assessment Program dataset, National Center for Atmospheric Research Earth System Grid data portal, Boulder, CO. Data downloaded 2010-03-25.
[<http://www.earthsystemgrid.org/browse/viewProject.htm?projectId=ff3949c8-2008-45c8-8e27-5834f54be50f>]
- Mearns, L. O., W. Gutowski, R. Jones, R. Leung, S. McGinnis, A Nunes, and Y. Qian, 2009: A regional climate change assessment program for North America, *Eos Trans. AGU*, 90 (36), 311.
- Meehl, G. A., et al. 2007: The WCRP CMIP3 multi-model dataset: A new era in climate change research, *Bull. Am. Meteorol. Soc.*, 88, 1383– 1394.
- Milly, P. C. D., Dunne, K. A., and Vecchia, A. V., 2005: Global patterns of trends in streamflow and water availability in a changing climate, *Nature*, 438, 347–350.
- Mote, P. W., 2006: Climate driven variability and trends in mountain snowpack in western North America. *J. of Climate*, 19, 6209-6220.
- Nakićenović, N., and R. Swart (eds.), 2000: Special Report on Emissions Scenarios. A Special Report of Working Group III of the Intergovernmental Panel on Climate Change. Cambridge University Press, Cambridge, United Kingdom and New York, NY, USA, 599 pp.
- Nijssen, B., G. M. O'Donnell, A. F. Hamlet, and D. P. Lettenmaier, 2001: Hydrologic vulnerability of global rivers to climate change. *Clim. Change*, 50, 143-175.
- Plummer D. A., D. Caya, A. Frigon, H. Côté, M. Giguère, D. Paquin, S. Biner, R. Harvey, R. de Elia, 2006: Climate and Climate Change over North America as Simulated by the Canadian RCM, *Journal of Climate*, 19, 3112-3132
- Randall, D.A., R.A. Wood, S. Bony, R. Colman, T. Fichefet, J. Fyfe, V. Kattsov, A. Pitman, J. Shukla, J. Srinivasan, R.J. Stouffer, A. Sumi and K.E. Taylor, 2007: Climate Models and Their Evaluation. In: *Climate Change 2007: The Physical Science Basis. Contribution of Working Group I to the*

- Fourth Assessment Report of the Intergovernmental Panel on Climate Change [Solomon, S., D. Qin, M. Manning, Z. Chen, M. Marquis, K.B. Averyt, M. Tignor and H.L. Miller (eds.)]. Cambridge University Press, Cambridge, United Kingdom and New York, NY, USA
- Seager, R., Ting, M., Held, I., Kushnir, Y., Lu, J., Vecchi, G., Huang, H.-P., Harnik, N., Leetmaa, A., Lau, N.-C., Li, C., Velez, J., and Naik, N., 2007: Model projections of an imminent transition to a more arid climate in southwestern North America, *Science Express*, 316, 1181–1184, doi:10.1126/science.1139601.
- Skamarock, W. C., J. B. Klemp, J. Dudhia, D. O. Gill, D. M. Barker, W. Wang, and J. G. Powers, 2005: A description of the Advanced Research WRF, Version 2. NCAR Technical Note 468+STR, National Center for Atmospheric Research, Boulder, CO. (Available at: http://wrf-model.org/wrfadmin/docs/arw_v2.pdf)
- Snyder M. A. and L. C. Sloan, 2005: Transient Future Climate over the Western United States Using a Regional Climate Model, *Earth Interactions*, 9, 1-21
- Stewart, I. T., 2009: Changes in snowpack and snowmelt runoff for key mountain regions. *Hydrological Process.*, 23, 78-94.
- Stewart, I. T., D. R. Cayan, and M. D. Dettinger, 2005: Changes toward earlier streamflow timing across western North America. *J. Climate*, 18, 1136–1155.
- Sushama, L., R. Laprise, D. Caya, A. Frigon and M. Slivitzky, 2006: Canadian RCM Projected Climate-Change Signal and its Sensitivity to Model Errors. *Int. J. Climatol.*, 26: 2141–2159. doi: 10.1002/joc.1362
- USCCSP Subcommittee on Global Change Research, 2007: Our changing planet. The US Climate Change Science Program for Fiscal Year 2007. Climate Change Science Program, Washington DC, pp 22–25
- Wang Shih-Yu, Robert R. Gillies, Eugene S. Takle, and William J. Gutowski Jr., 2009: Evaluation of precipitation in the Intermountain Region as simulated by the NARCCAP regional climate models, *Geophys. Res. Lett.*, 36, L11704, doi:10.1029/2009GL037930.
- Zhang Y, V Dulière, P Mote, EP Salathé 2009: Evaluation of WRF and HadRM Mesoscale Climate

Simulations over the United States Pacific Northwest. *J. Climate*, 22, 5511-5526.

Figures list

Figure 1 Location (left) and topography distribution (center; unit: m) and histogram of topography (right) for the Colorado River basin.

Figure 2 Surface air temperature distribution pattern for current period (1970-1999) of the 1/8-degree historical NLDAS data set (NLDAS), RCMs/GCMs combinations (left), the host GCMs (center) and difference between the RCMs and its host GCMs (RCMs-GCMs, right).

Figure 3 Variations in annual, winter, spring, and summer surface air temperature as elevation from the RCMs/GCMs and the host GCMs comparing to the 1/8-degree historical NLDAS data set (NLDAS) over the CRB (the solid line is the historical period and the dash line is the future period).

Figure 4 Similar to Figure 2, but for precipitation.

Figure 5 Similar to Figure 3, but for annual, winter, and summer precipitation.

Figure 6 Similar to Figure 2, but for evapotranspiration.

Figure 7 Similar to Figure 5, but for evapotranspiration.

Figure 8. Similar to Figure 2, but for runoff.

Figure 9 Similar to Figure 3, but for runoff.

Figure 10 Annual snow water equivalent distribution and annual, winter and spring variations as elevation from the RCMs/GCMs and the host GCMs comparing to the 1/8-degree historical NLDAS data set (NLDAS) over the CRB (the solid line is the historical period and the dash line is the future period). Results for HadCM3 not archived.

Figure 11 Similar to Figure 5, but for terrestrial storage change.

Figure 12 The distribution (left) and basin average (right) of annual, and seasonal surface air temperature (T) change over the CRB for the RCMs and the host GCMs for the future (2040-2069) minus current (1970-1999).

Figure 13 Similar to Figure 12, but for runoff (R) change.

Figure 14 The distribution of winter and summer precipitation (P) change for the RCMs and their host GCMs for the future (2040-2069) minus current (1970-1999).

Figure 15. The distribution of winter and spring snow water equivalent (SWE) change for the RCMs and the host GCMs for the future (2040-2069) minus current (1970-1999). Results for HadCM3 not archived.

Figure 16 Similar to Figure 13, but at 2.5-degree resolution.

Tables list:

Table 1 Status of NARCCAP archived RCM/GCM combinations.

Table 2 Forcing Global Climate Model (GCMs) runs chosen for the NARCCAP Phase II multiple regional climate model (RCMs) runs for current (20C3M; 1970-1999) and future (A2; 2040-2069) scenarios.

Table 3 Annual (ANN) and seasonal (DJF, MAM, JJA and SON) NLDAS and simulation of the surface air temperature (T), precipitation (P), evapotranspiration (ET), runoff (R), terrestrial storage change (P-ET-R) and snow water equivalent (SWE) for the RCM driven by GCM (RCM/GCM) and GCM over the CRB for 1970-1999 and spatial correlation coefficient (CORR) between RCMs, GCMs, and NLDAS. T is in units of °C and P, ET, R, and P-ET-R are in units of $\text{mm} \cdot \text{d}^{-1}$, SWE are in units of mm.

Table 3.1 Biases of surface air temperature for the RCM simulations. $\text{Bias}_{\text{phys}}$ is the biases of the RCM simulations forced by NCEP/DOE, which represents the bias from physics processes; $\text{Bias}_{\text{total}}$ is from the RCM simulations forced by GCMs, which represents the bias from physics processes and forcing GCM. Contr is the absolute of $\text{bias}_{\text{phys}}$ divided by the absolute of $\text{bias}_{\text{total}}$, which represents the contribution of bias from physics processes. RCM3^1 is RCM3 forced by CGCM3; RCM3^2 is RCM3 forced by GFDL.

Table 4 Annual and seasonal precipitation (P) change (2040-2069)-(1970-1999) for RCMs and GCMs over the CRB (unit: $\text{mm} \cdot \text{d}^{-1}$ (%))

Table 5 Similar to Table 4, but for evapotranspiration (ET) change (unit: $\text{mm} \cdot \text{d}^{-1}$ (%))

Table 6 Similar to Table 4, but for runoff (R) change spatial averaged over area above 2250 m (unit: $\text{mm} \cdot \text{d}^{-1}$ (%))

Table 7 Similar to Table 4, but for snow water equivalent (SWE) change (unit: mm (%)).

Table 8 Annual and seasonal surface air temperature (T) (T change, (2040-2069)-(1970-1999)) for area above 2250 m for RCMs and GCMs (unit: °C)

Table 9 Intermodal standard deviation, as a measure of uncertainty, over CRB for temperature (°C), precipitation ($\text{mm} \cdot \text{d}^{-1}$), and runoff ($\text{mm} \cdot \text{d}^{-1}$) for the RCMs and GCMs projection

Table 1 Status of NARCCAP archived RCM/GCM combinations.

	GFDL	Phase II			Phase I
		CGCM3	HadCM3	CCSM3	NCEP/DOE
CRCM	--	finished	--	planned	finished
ECPC	running	--	planned	--	finished
HRM3	planned	--	finished	--	finished
MM5	--	--	planned	running	finished
RCM3	finished	finished	--	--	finished
WRF	--	planned	--	finished	finished

Table 2 Forcing Global Climate Model (GCMs) runs chosen for the NARCCAP Phase II multiple regional climate model (RCMs) runs for current (20C3M; 1970-1999) and future (A2; 2040-2069) scenarios.

GCM	Scenario	PCMDI/CMIP3	Notes
CCSM3	current	ncar_ccsm3_0 20c3m	Run5
	future	ncar_ccsm3_0 sresa2	Run5
CGCM3	current	cccma_cgcm3_1 20c3m	Run4
	future	cccma_cgcm3_1 sresa2	Run4
HadCM3	current	Not archived	Custom run for
	future	Not archived	NARCCAP
GFDL	current	gfdl_cm2_1 20c3m	Run2
	future	gfdl_cm2_1 sresa2	Run1

Table 3 Annual (ANN) and seasonal (DJF, MAM, JJA and SON) NLDAS and simulation of the surface air temperature (T), precipitation (P), evapotranspiration (ET), runoff (R), terrestrial storage change (P-ET-R) and snow water equivalent (SWE) for the RCM driven by GCM (RCM/GCM) and GCM over the CRB for 1970-1999 and spatial correlation coefficient (CORR) between RCMs, GCMs, and NLDAS. T is in units of °C and P, ET, R, and P-ET-R are in units of mm · d⁻¹, SWE are in units of mm.

		Value					CORR				
		ANN	DJF	MAM	JJA	SON	ANN	DJF	MAM	JJA	SON
T	NLDAS	10.65	0.37	9.77	21.33	11.27	1	1	1	1	1
	WRF/CCSM3	9.15	-2.11	8.86	20.86	8.99	0.95	0.96	0.94	0.93	0.95
	MM5/CCSM3	9.63	-1.42	9.44	21.35	9.13	0.95	0.96	0.94	0.92	0.95
	CCSM3	10.34	-1.66	8.62	23.88	10.51	0.88	0.92	0.85	0.82	0.89
	CRCM/CGCM3	7.52	-4.21	6.67	20.46	7.15	0.94	0.96	0.93	0.91	0.94
	RCM3/CGCM3	7.45	-3.78	5.77	19.81	7.98	0.94	0.95	0.93	0.91	0.94
	CGCM3	9.5	-3.33	7.58	23.47	10.29	0.86	0.91	0.84	0.8	0.88
	RCM3/GFDL	6.03	-5.28	3.39	19.11	6.89	0.94	0.95	0.93	0.92	0.94
	GFDL	8.32	-3.58	6.43	21.93	8.49	0.87	0.91	0.84	0.82	0.89
	HRM3/HadCM3	12.1	0.16	9.79	25.6	12.87	0.95	0.96	0.94	0.92	0.95
HadCM3	11.26	-0.92	9.5	24.56	11.89	0.88	0.92	0.84	0.83	0.89	
P	NLDAS	1.01	1.04	0.93	1.02	1.05	1	1	1	1	1
	WRF/CCSM3	0.91	1.62	0.98	0.36	0.69	0.72	0.56	0.75	0.43	0.7
	MM5/CCSM3	1.09	1.92	1.1	0.34	0.99	0.73	0.64	0.78	0.42	0.75
	CCSM3	1.14	1.91	1.18	0.44	1.05	0.22	-0.18	0.47	0.55	0.33
	CRCM/CGCM3	0.99	1.1	1.09	0.83	0.95	0.62	0.47	0.68	0.58	0.63
	RCM3/CGCM3	1.17	1.64	1.24	0.57	1.24	0.6	0.49	0.74	0.47	0.59
	CGCM3	0.98	1.19	1.01	0.76	0.97	0.4	-0.08	0.62	0.37	0.49
	RCM3/GFDL	1.86	2.35	1.84	1.12	2.11	0.65	0.51	0.65	0.51	0.6
	GFDL	1.61	2.01	1.61	0.97	1.84	0.34	-0.24	0.51	0.2	0.22
	HRM3/HadCM3	1.35	1.63	1.69	1.18	0.89	0.62	0.53	0.7	0.62	0.64
HadCM3	1.39	1.53	1.78	1.26	0.98	0.31	-0.11	0.54	0.42	0.41	
ET	NLDAS	0.87	0.36	0.85	1.59	0.69	1	1	1	1	1
	WRF/CCSM3	0.78	0.5	1.16	1.1	0.34	0.71	0.54	0.68	0.7	0.55
	CCSM3	0.65	0.44	1.03	0.57	0.58	0.48	0.68	0.43	0.34	0.47
	CRCM/CGCM3	0.82	0.39	1.28	1.02	0.59	0.56	0.6	0.34	0.55	0.58
	CGCM3	0.81	0.46	1.27	0.88	0.63	0.5	0.53	0.23	0.43	0.54
	HRM3/HadCM3	1.09	0.6	1.66	1.57	0.55	0.59	0.49	0.51	0.61	0.58
	HadCM3	1.29	0.65	2.02	1.76	0.72	0.34	0.36	0.22	0.4	0.48
	NLDAS	0.15	0.09	0.21	0.22	0.07	1	1	1	1	1
WRF/CCSM3	0.15	0.2	0.33	0.04	0.03	0.16	0.24	0.26	0	-0.11	
CCSM3	0.43	0.72	0.8	0.06	0.13	-0.02	-0.15	0.19	0.1	-0.15	
CRCM/CGCM3	0.17	0.08	0.6	0.01	0	0.5	-0.25	0.56	0.31	0.32	
CGCM3	0.18	0.14	0.56	0	0	0.26	-0.19	0.3	0.28	0.2	
HRM3/HadCM3	0.25	0.09	0.67	0.2	0.06	0.47	0.2	0.45	0.41	0.5	
HadCM3	0.1	0.04	0.17	0.13	0.05	0.08	-0.22	0.07	0.11	0.03	
P-ET-R	NLDAS	-0.01	0.59	-0.13	-0.79	0.29	1	1	1	1	1
	WRF/CCSM3	-0.02	0.92	-0.52	-0.78	0.32	0.01	0.53	0.33	0.65	0.62
	CCSM3	0.06	0.75	-0.65	-0.19	0.33	0.1	0.06	-0.37	0.24	0.46
	CRCM/CGCM3	0	0.64	-0.78	-0.2	0.36	-0.24	0.47	-0.31	0.54	0.62
	CGCM3	0	0.59	-0.82	-0.12	0.34	0.16	0.16	-0.45	0.34	0.38
	HRM3/HadCM3	0	0.95	-0.64	-0.59	0.28	-0.19	0.53	-0.18	0.65	0.61
	HadCM3	0	0.84	-0.41	-0.63	0.21	0.08	0.06	0.5	0.39	0.31
	NLDAS	14.95	24.51	28.68	3.97	2.63	1	1	1	1	1
WRF/CCSM3	5.82	16.48	5.72	0	1.05	0.47	0.56	0.47	--	--	
CCSM3	19.96	29.92	25.9	0	4.52	0.21	0.31	0.21	--	--	
CRCM/CGCM3	16.72	38.34	25.67	0.06	2.83	0.47	0.53	0.59	--	--	
CGCM3	11.25	29.39	14.23	0	1.4	0.28	0.36	0.30	--	--	
HRM3/HadCM3	13.66	31.68	21.26	0.05	1.63	0.42	0.53	0.44	--	--	
HadCM3				Not reported					Not reported		

Table 3.1 Biases of surface air temperature for the RCM simulations. $Bias_{phys}$ is the biases of the RCM simulations forced by NCEP/DOE, which represents the bias from physics processes; $Bias_{total}$ is from the RCM simulations forced by GCMs, which represents the bias from physics processes and forcing GCM. Contr is the absolute of $bias_{phys}$ divided by the absolute of $bias_{total}$, which represents the contribution of bias from physics processes. RCM3¹ is RCM3 forced by CGCM3; RCM3² is RCM3 forced by GFDL.

	$Bias_{phys}$ (°C)	$bias_{total}$ (°C)	Contr(%)
WRF	0.07	-1.5	4
MM5	0	-1.02	0
CRCM	-1.26	-3.13	40
RCM3 ¹	0.18	-3.2	5
RCM3 ²	0.18	-4.62	4
HRM3	4.33	1.45	60

Table 4 Annual and seasonal precipitation (P) change (2040-2069)-(1970-1999) for RCMs and GCMs over the CRB (unit: mm · d⁻¹ (%))

	ANN		DJF		MAM		JJA		SON	
WRF	-0.03	(-3%)	0.00	(0%)	-0.04	(-4%)	-0.04	(-11%)	-0.03	(-4%)
CCSM3	-0.06	(-5%)	-0.12	(-6%)	-0.11	(-9%)	0.13	(30%)	-0.14	(-13%)
CRCM	-0.09	(-9%)	0.04	(4%)	-0.13	(-12%)	-0.22	(-27%)	-0.03	(-3%)
CGCM3	-0.01	(-1%)	0.10	(8%)	-0.06	(-6%)	-0.07	(-9%)	-0.02	(-2%)
HRM3	-0.06	(-4%)	0.08	(5%)	-0.14	(-8%)	-0.24	(-20%)	0.07	(8%)
HadCM3	0.01	(1%)	0.11	(7%)	-0.19	(-11%)	-0.05	(-4%)	0.16	(16%)

Table 5 Similar to Table 4, but for evapotranspiration (ET) change (unit: $\text{mm} \cdot \text{d}^{-1}$ (%))

	ANN		DJF		MAM		JJA		SON	
WRF	0	(0%)	0.04	(8%)	0.02	(2%)	-0.09	(-8%)	0.05	(15%)
CCSM3	0.06	(9%)	0.11	(25%)	0.03	(3%)	0.09	(16%)	0.02	(3%)
CRCM	-0.05	(-6%)	0.09	(23%)	0	(0%)	-0.23	(-23%)	-0.06	(-10%)
CGCM3	0.02	(2%)	0.09	(20%)	0.05	(4%)	-0.03	(-3%)	-0.03	(-5%)
HRM3	-0.07	(-6%)	0.04	(7%)	-0.05	(-3%)	-0.28	(-18%)	0.02	(4%)
HadCM3	-0.01	(-1%)	0.05	(8%)	-0.09	(-4%)	-0.14	(-8%)	0.12	(17%)

Table 6 Similar to Table 4, but for runoff (R) change spatial averaged over area above 2250 m (unit: $\text{mm} \cdot \text{d}^{-1}$ (%))

	ANN		DJF		MAM		JJA		SON	
WRF	-0.03	(-16%)	0	(0%)	-0.11	(-19%)	0	(0%)	0	(0%)
CCSM3	-0.07	(-16%)	0.27	(61%)	-0.56	(-50%)	0.01	(17%)	0	(0%)
CRCM	-0.07	(-16%)	0.06	(200%)	-0.32	(-19%)	-0.03	(-75%)	0	(0%)
CGCM3	-0.04	(-13%)	0.12	(80%)	-0.3	(-27%)	0.01	(100%)	0	(0%)
HRM3	0.05	(5%)	0.15	(88%)	0.2	(7%)	-0.15	(-20%)	0.01	(5%)
HadCM3	0.01	(6%)	0.01	(20%)	0.04	(15%)	-0.02	(-9%)	0	(0%)

Table 7 Similar to Table 4, but for snow water equivalent (SWE) change (unit: mm (%)).

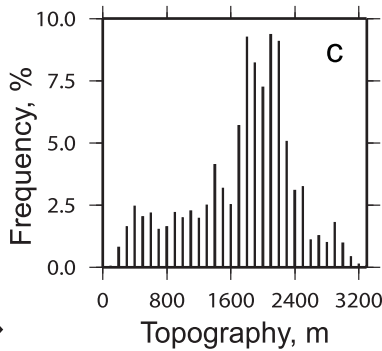
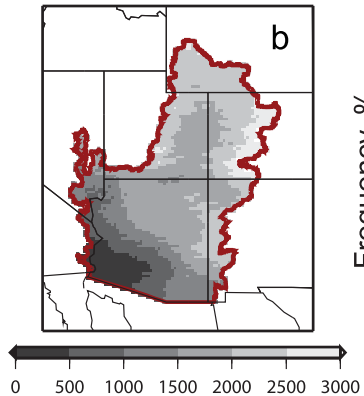
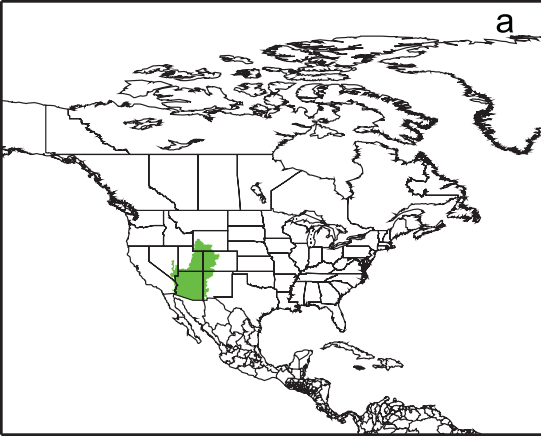
	ANN		DJF		MAM		JJA		SON	
WRF	-1.9	(-32%)	-4.5	(-27%)	-2.3	(-41%)	--	--	--	--
CCSM3	-11.3	(-57%)	-15.4	(-51%)	-18.9	(-73%)	--	--	--	--
CRCM	-4.3	(-26%)	-7.9	(-21%)	-8.4	(-33%)	--	--	--	--
CGCM3	-4.0	(-36%)	-8.4	(-28%)	-7.2	(-50%)	--	--	--	--
HRM3	-3.8	(-28%)	-7.7	(-24%)	-6.7	(-32%)	--	--	--	--
HadCM3	Not reported									

Table 8 Annual and seasonal surface air temperature (T) (T change, (2040-2069)-(1970-1999)) for area above 2250 m for RCMs and GCMs (unit: °C)

	ANN		DJF		MAM		JJA		SON	
WRF	1.6	(2.71)	-9.71	(2.52)	1.16	(2.29)	13.49	(3.12)	1.44	(2.89)
CCSM3	5.26	(3.3)	-7.5	(2.85)	3.13	(3.4)	20.11	(3.73)	5.32	(3.21)
CRCM	0.11	(2.9)	-12.02	(2.75)	-1.23	(2.32)	13.57	(3.52)	0.11	(3.03)
CGCM3	4.92	(2.67)	-7.81	(2.59)	2.52	(2.46)	19.15	(2.96)	5.8	(2.69)
HRM3	4.3	(2.92)	-7.4	(2.43)	1.62	(2.37)	17.65	(3.79)	5.33	(3.08)
HadCM3	6.99	(3.09)	-5.58	(2.96)	5.45	(2.52)	20.34	(3.72)	7.74	(3.15)

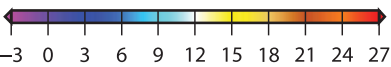
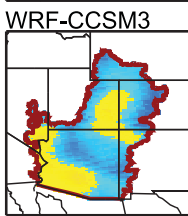
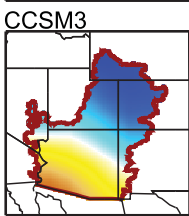
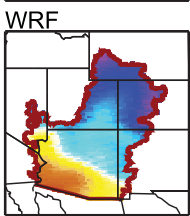
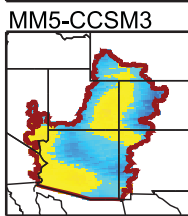
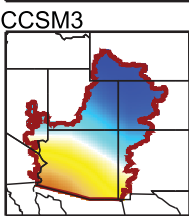
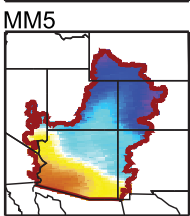
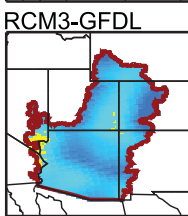
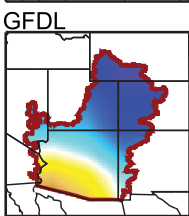
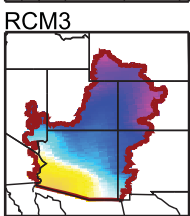
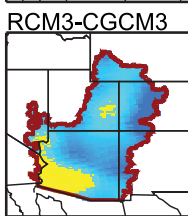
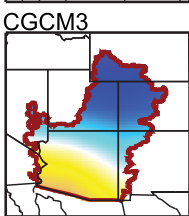
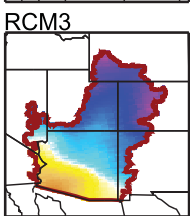
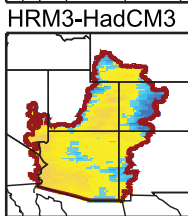
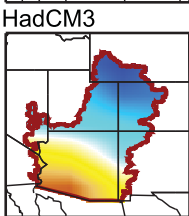
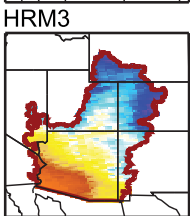
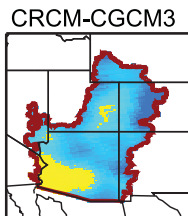
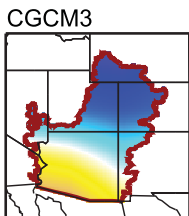
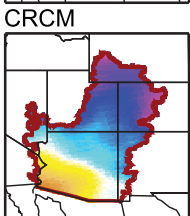
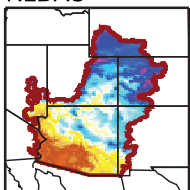
Table 9 Intermodal standard deviation, as a measure of uncertainty, over CRB for temperature (°C), precipitation (mm d⁻¹), and runoff (mm d⁻¹) for the RCMs and GCMs projection

		ANN	DJF	MAM	JJA	SON
T	RCM	0.29	0.08	0.35	0.57	0.35
	GCM	0.32	0.33	0.44	0.46	0.34
P	RCM	0.05	0.07	0.10	0.19	0.10
	GCM	0.06	0.23	0.11	0.19	0.26
R	RCM	0.05	0.07	0.17	0.02	0.01
	GCM	0.10	0.03	0.38	0.01	0.03

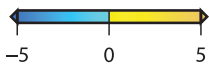


30-year mean temperature

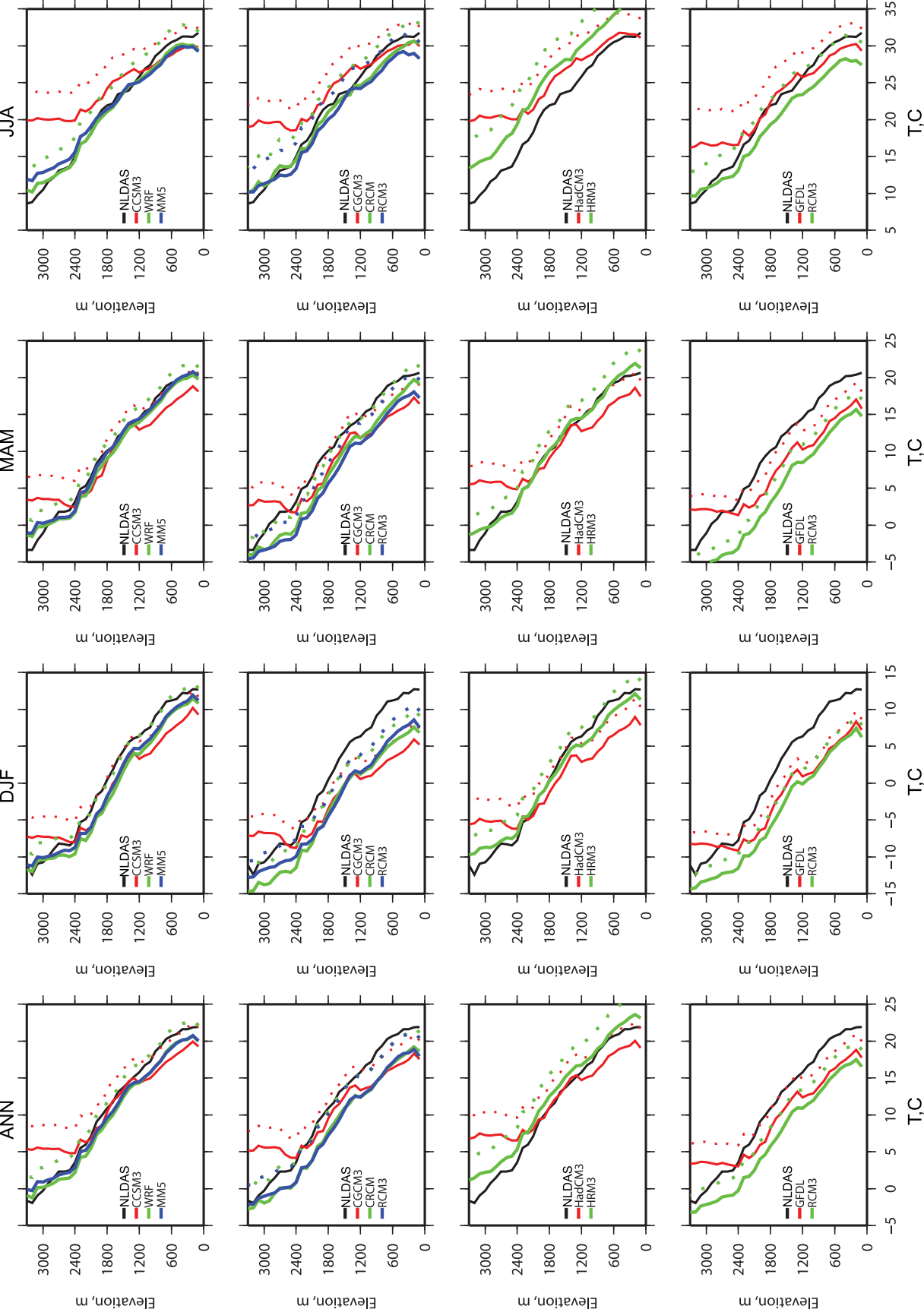
(1970–1999)



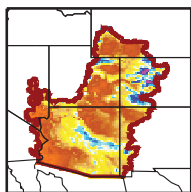
T (C)



T diff (C)



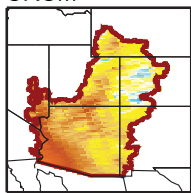
NLDAS



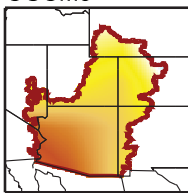
30_year mean precipitation

(1970-1999)

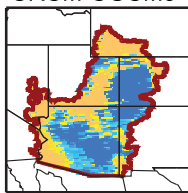
CRCM



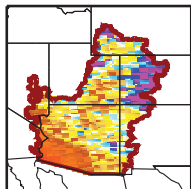
CGCM3



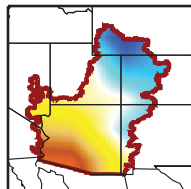
CRCM-CGCM3



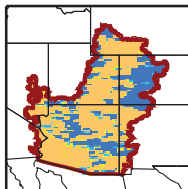
HRM3



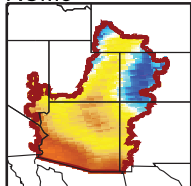
HadCM3



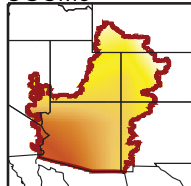
HRM3-HadCM3



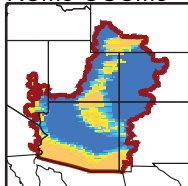
RCM3



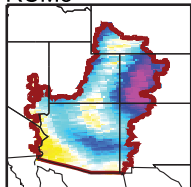
CGCM3



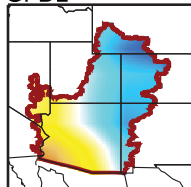
RCM3-CGCM3



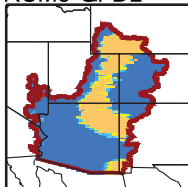
RCM3



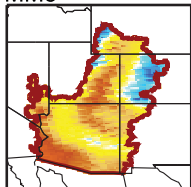
GFDL



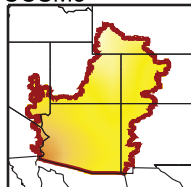
RCM3-GFDL



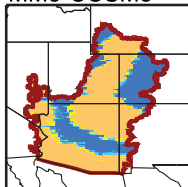
MM5



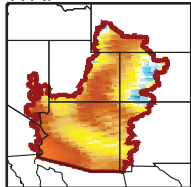
CCSM3



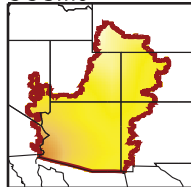
MM5-CCSM3



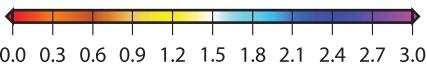
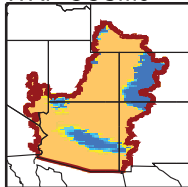
WRF



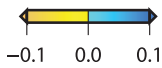
CCSM3



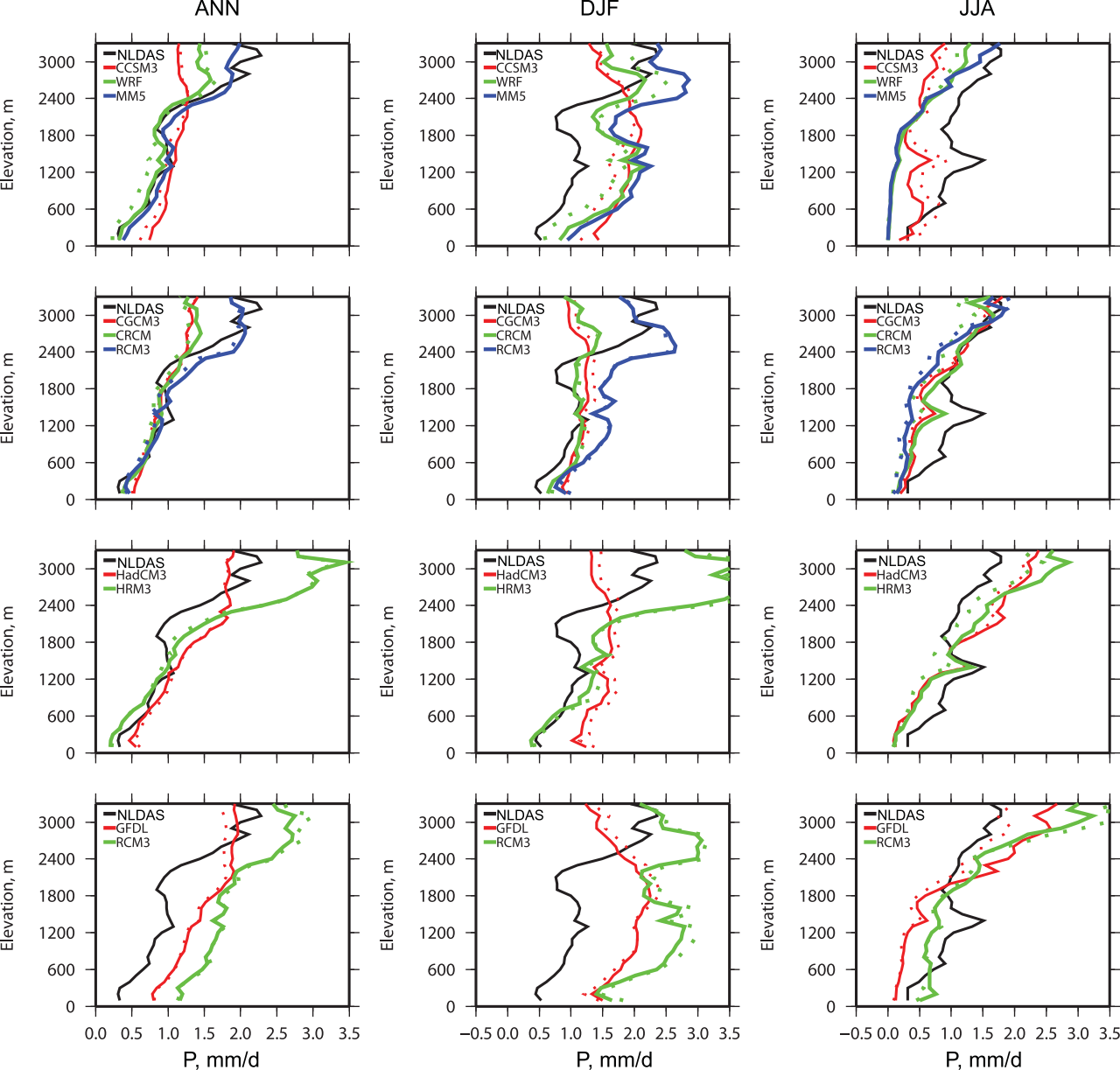
WRF-CCSM3



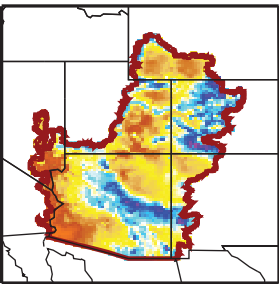
P (mm/d)



P diff (mm/d)



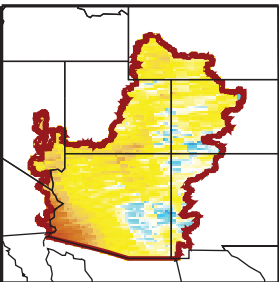
NLDAS



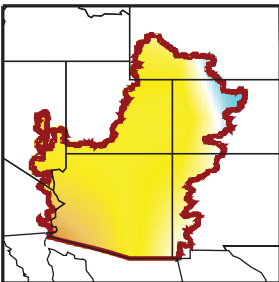
30-year mean evapotranspiration

(1970–1999)

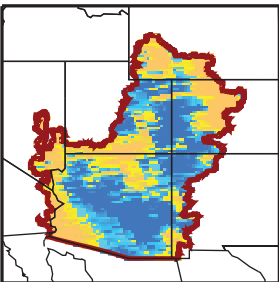
CRCM



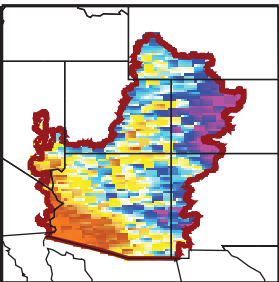
CGCM3



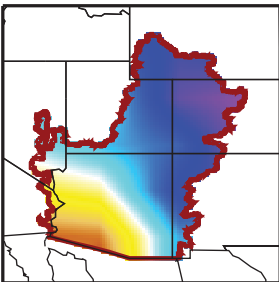
CRCM-CGCM3



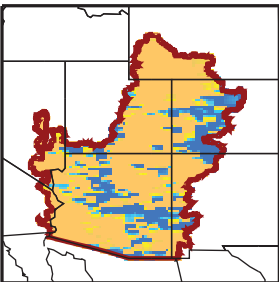
HRM3



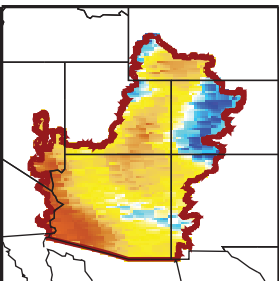
HadCM3



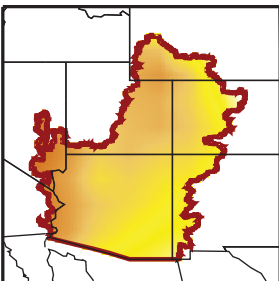
HRM3-HadCM3



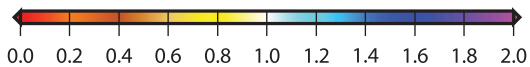
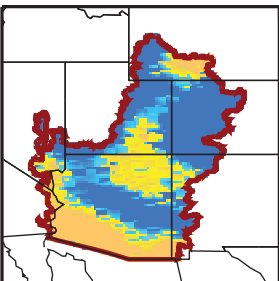
WRF



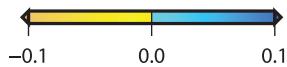
CCSM3



WRF-CCSM3

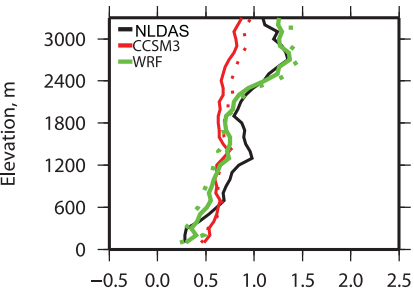


ET (mm/d)

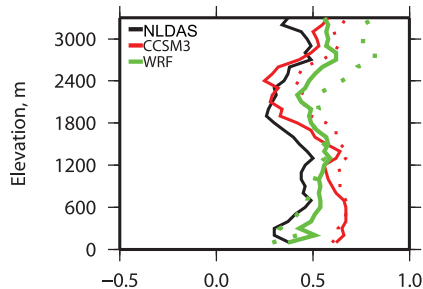


ET diff (mm/d)

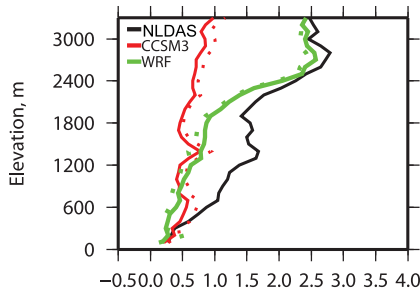
ANN



DJF



JJA



Elevation, m

Elevation, m

Elevation, m

Elevation, m

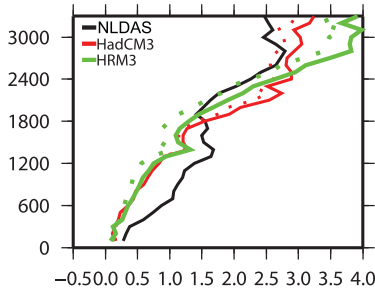
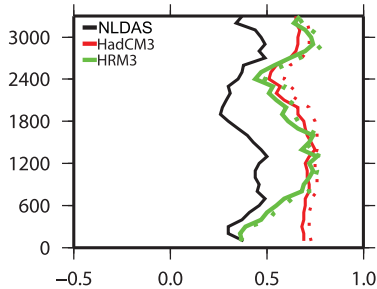
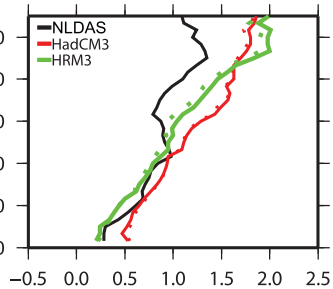
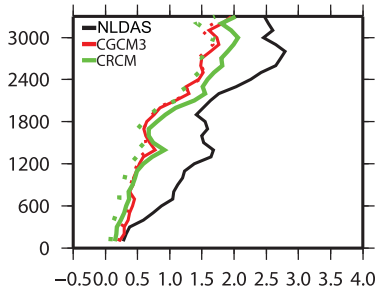
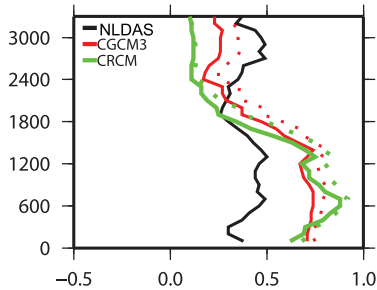
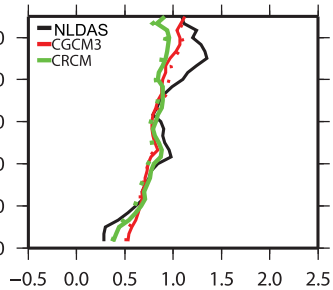
Elevation, m

Elevation, m

Elevation, m

Elevation, m

Elevation, m

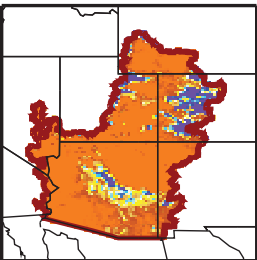


ET, mm/d

ET, mm/d

ET, mm/d

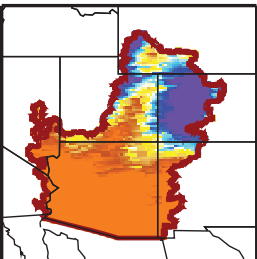
NLDAS



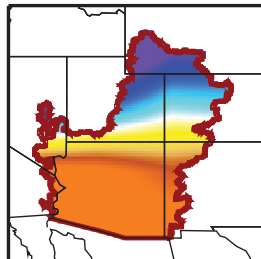
30-year mean Runoff

(1970–1999)

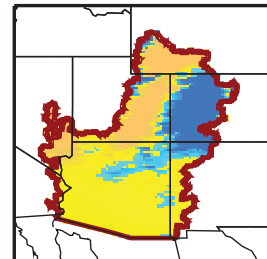
CRCM



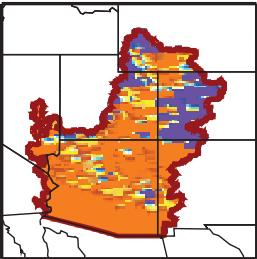
CGCM3



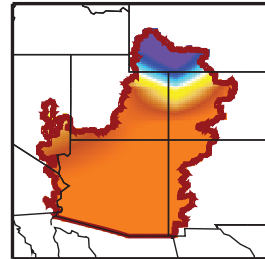
CRCM-CGCM3



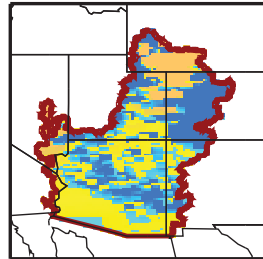
HRM3



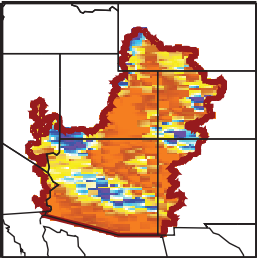
HadCM3



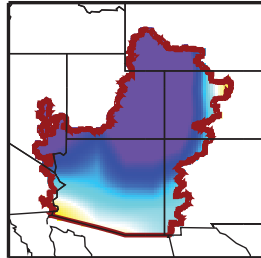
HRM3-HadCM3



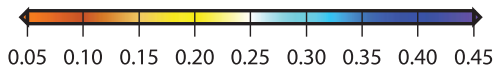
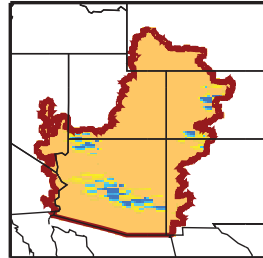
WRF



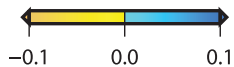
CCSM3



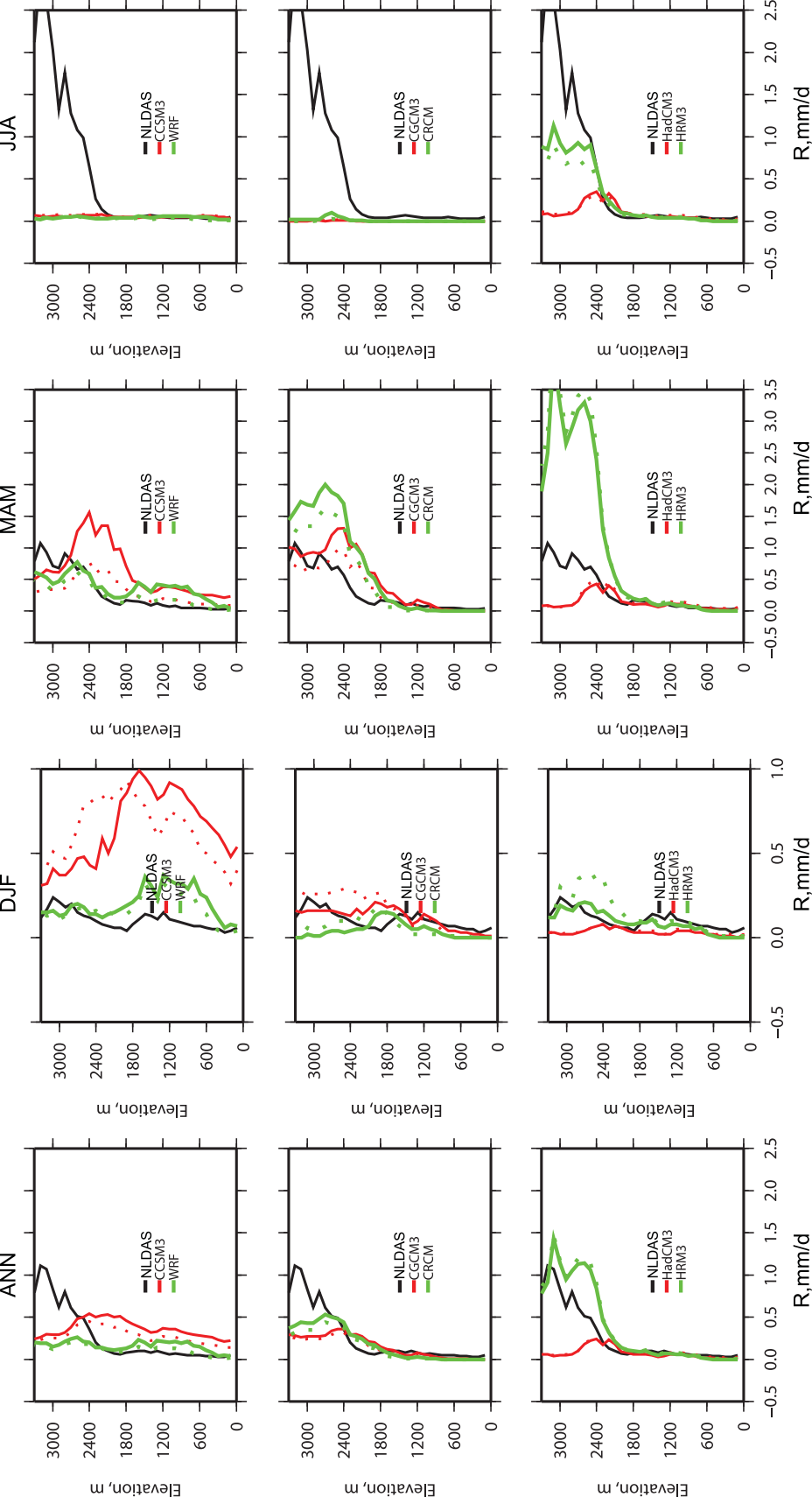
WRF-CCSM3

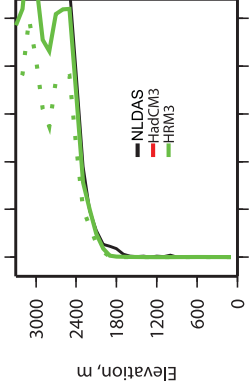
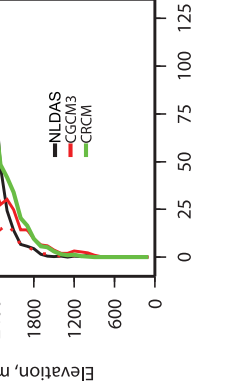
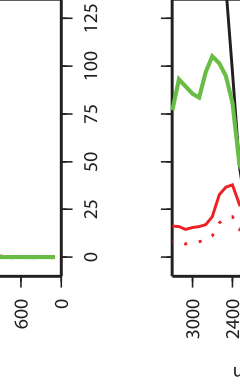
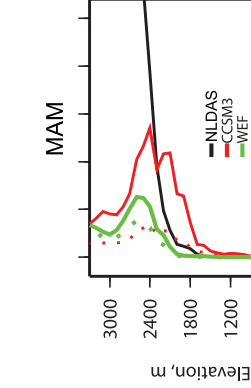
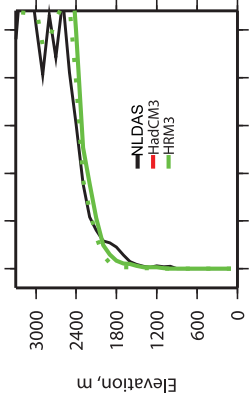
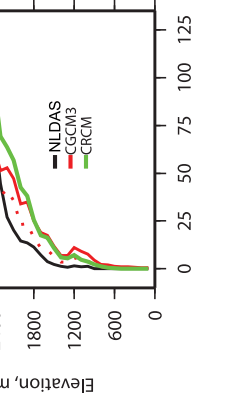
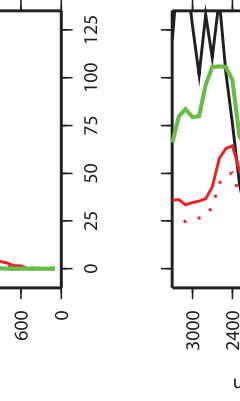
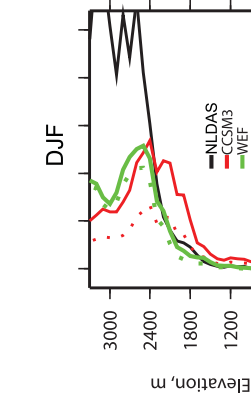
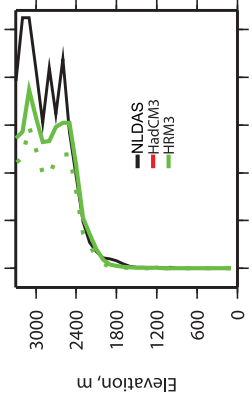
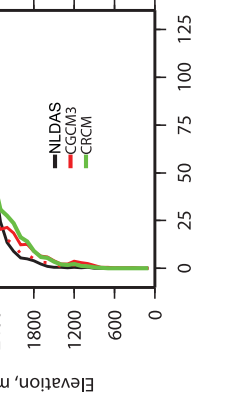
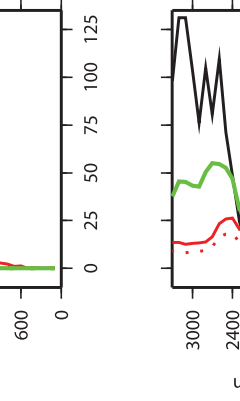
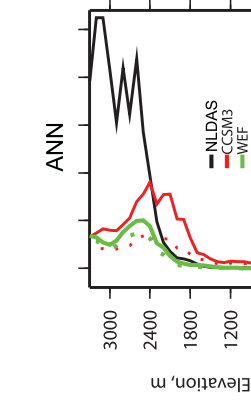
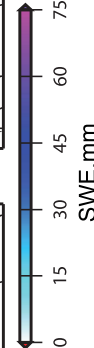
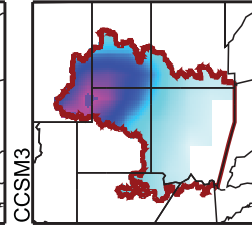
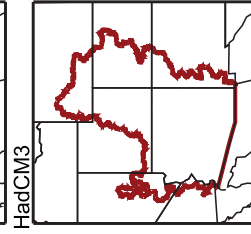
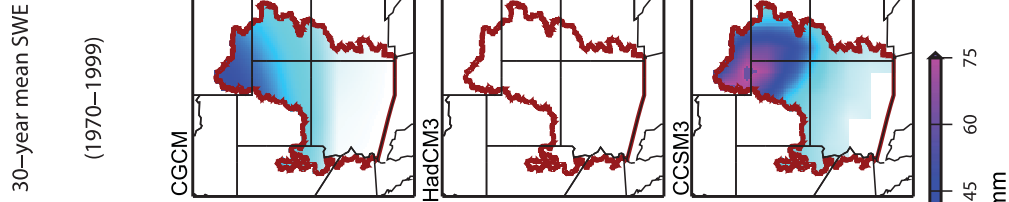
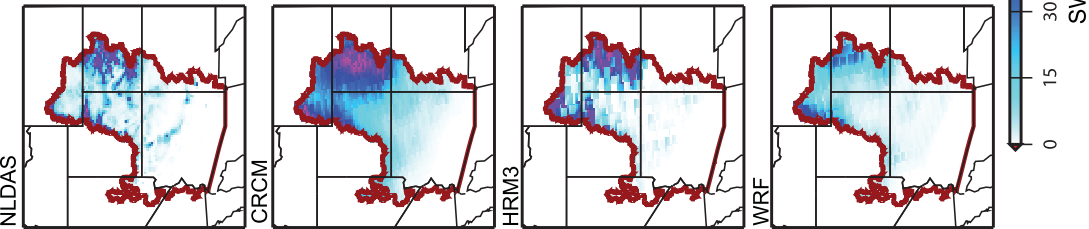


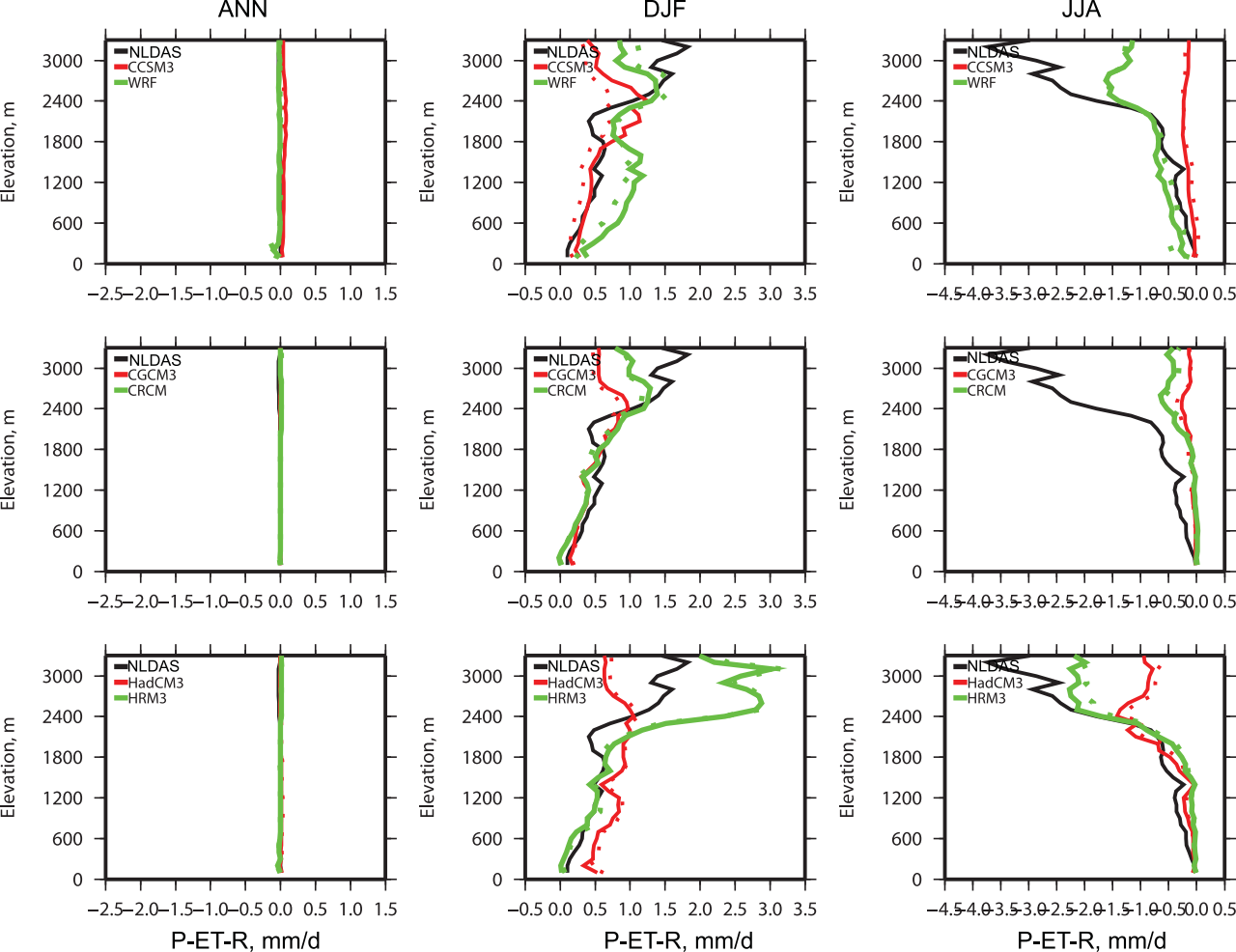
R (mm/d)



R diff (mm/d)



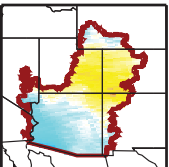




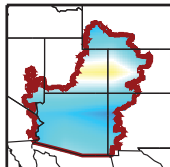
ANN

DJF

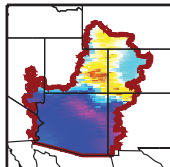
CRCM



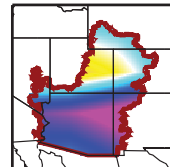
CGCM3



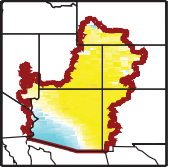
CRCM



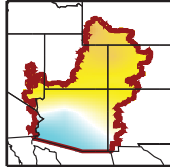
CGCM3



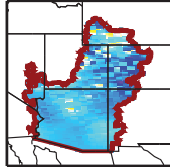
HRM3



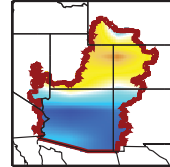
HadCM3



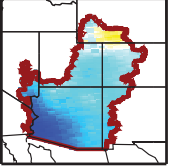
HRM3



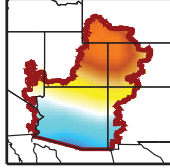
HadCM3



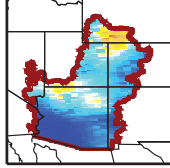
WRF



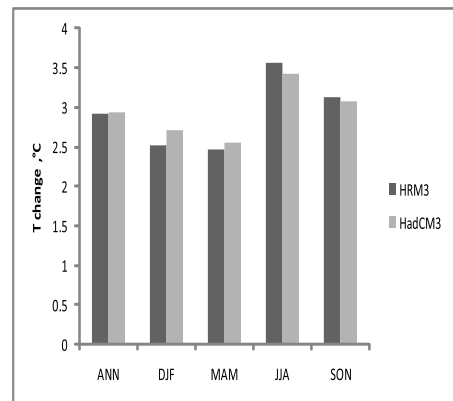
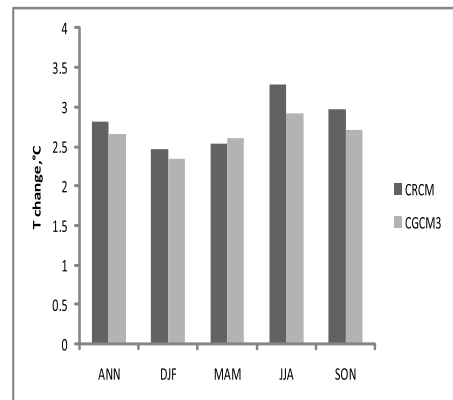
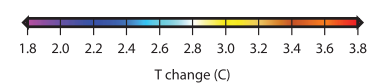
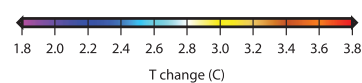
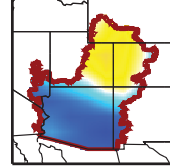
CCSM3



WRF



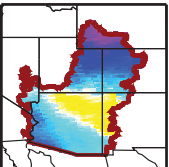
CCSM3



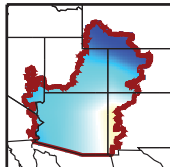
MAM

JJA

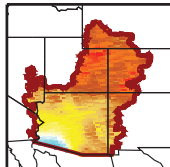
CRCM



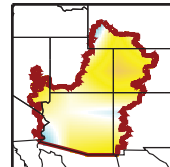
CGCM3



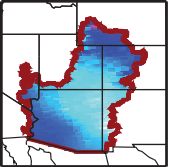
CRCM



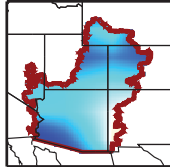
CGCM3



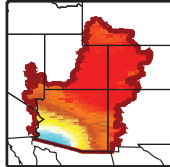
HRM3



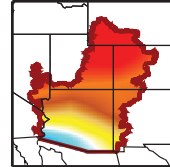
HadCM3



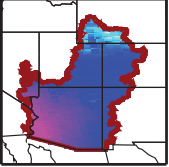
HRM3



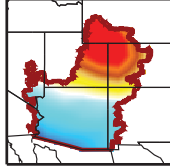
HadCM3



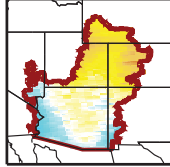
WRF



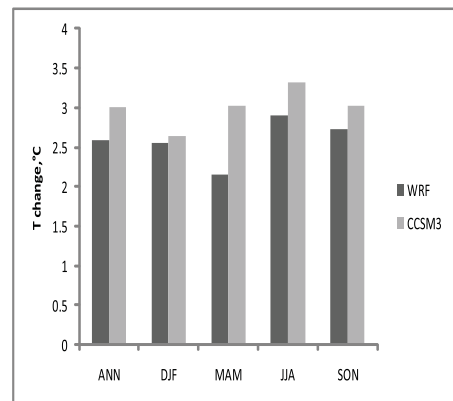
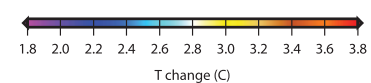
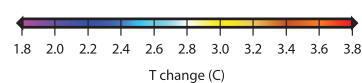
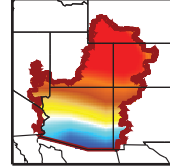
CCSM3



WRF



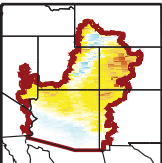
CCSM3



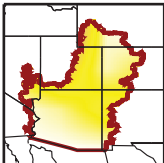
ANN

DJF

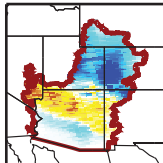
CRCM



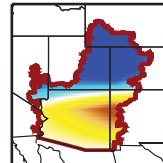
CGCM3



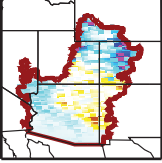
CRCM



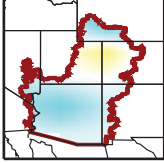
CGCM3



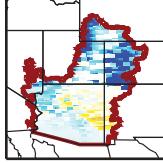
HRM3



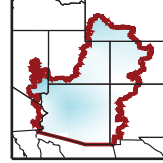
HadCM3



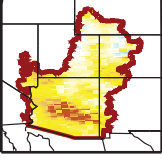
HRM3



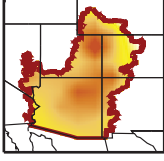
HadCM3



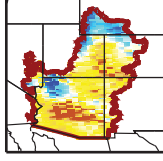
WRF



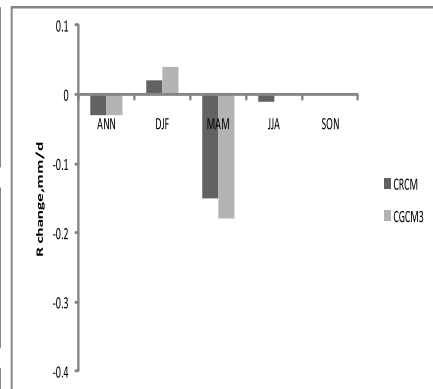
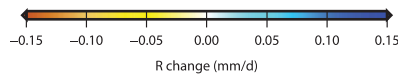
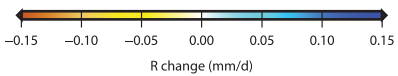
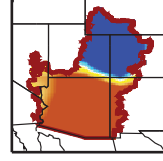
CCSM3



WRF



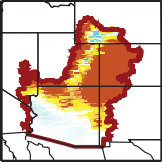
CCSM3



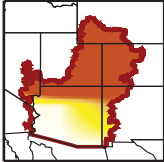
MAM

JJA

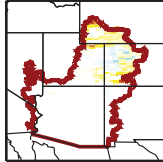
CRCM



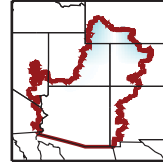
CGCM3



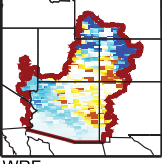
CRCM



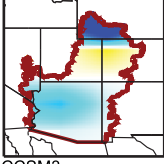
CGCM3



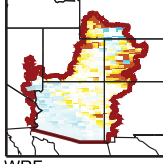
HRM3



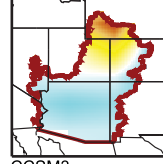
HadCM3



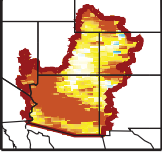
HRM3



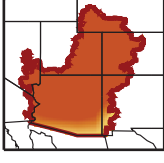
HadCM3



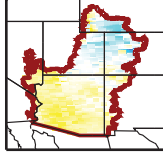
WRF



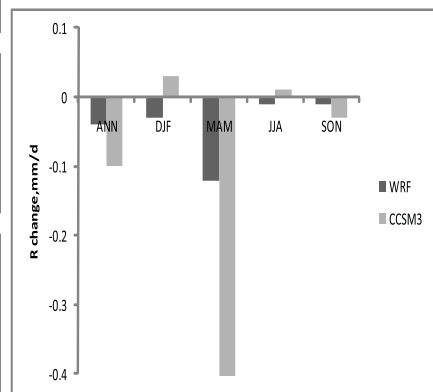
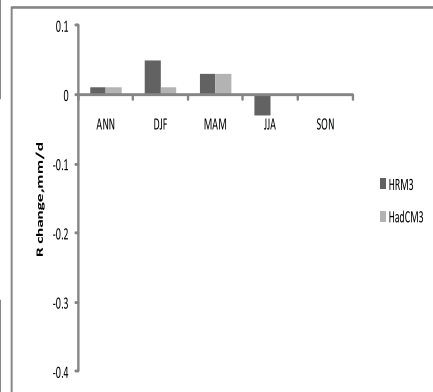
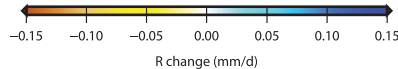
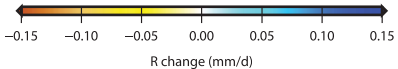
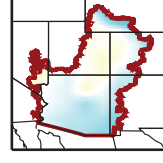
CCSM3



WRF



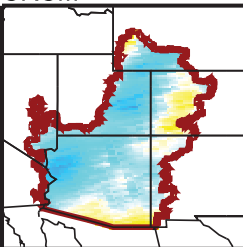
CCSM3



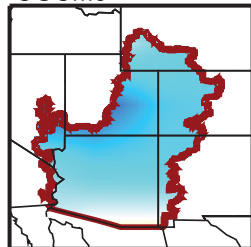
DJF

JJA

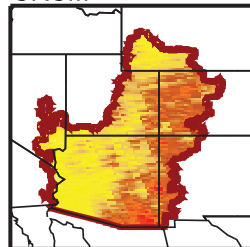
CRCM



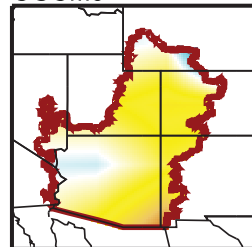
CGCM3



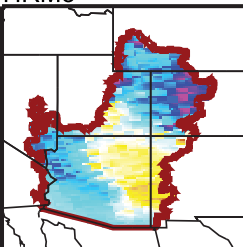
CRCM



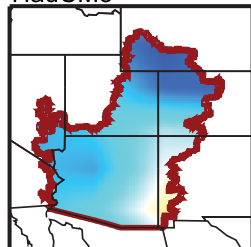
CGCM3



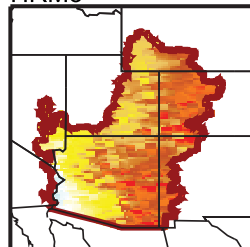
HRM3



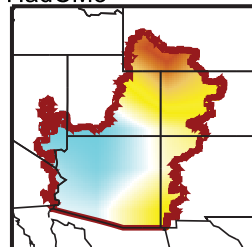
HadCM3



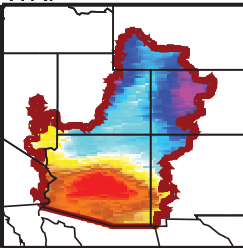
HRM3



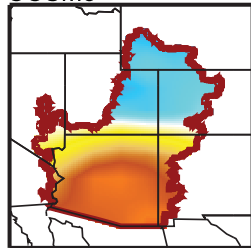
HadCM3



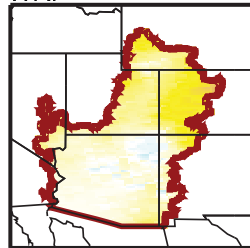
WRF



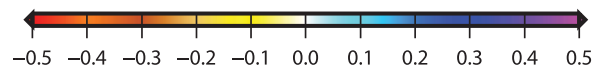
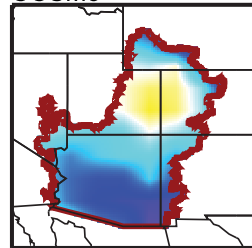
CCSM3



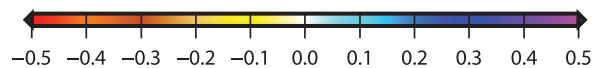
WRF



CCSM3



P change (mm/d)

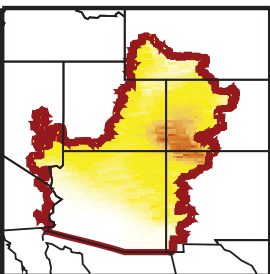


P change (mm/d)

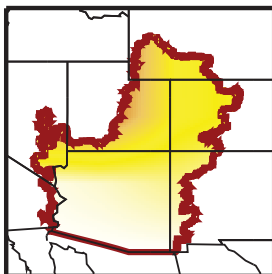
DJF

MAM

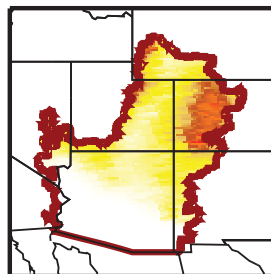
CRCM



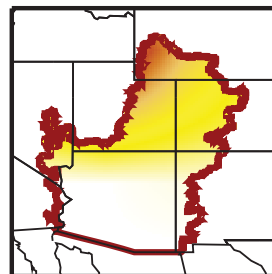
CGCM3



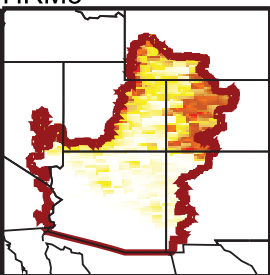
CRCM



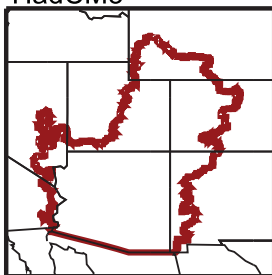
CGCM3



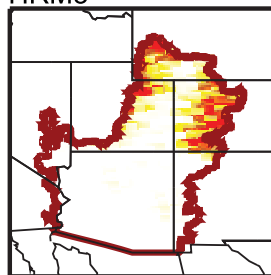
HRM3



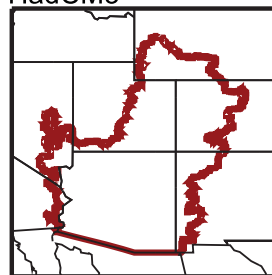
HadCM3



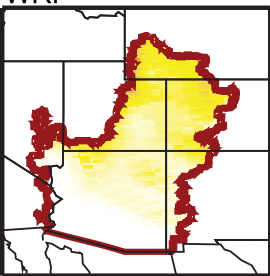
HRM3



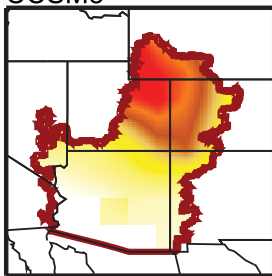
HadCM3



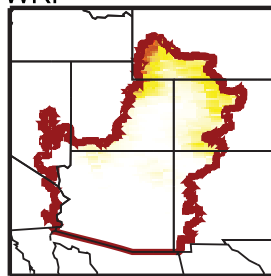
WRF



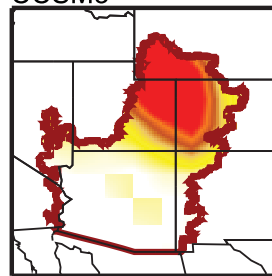
CCSM3



WRF



CCSM3



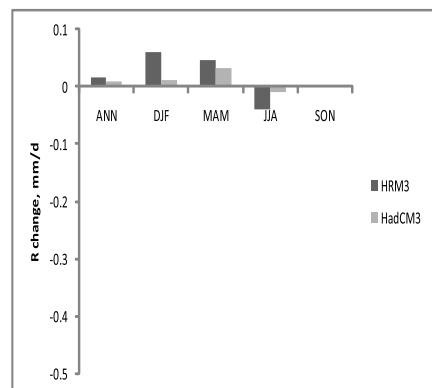
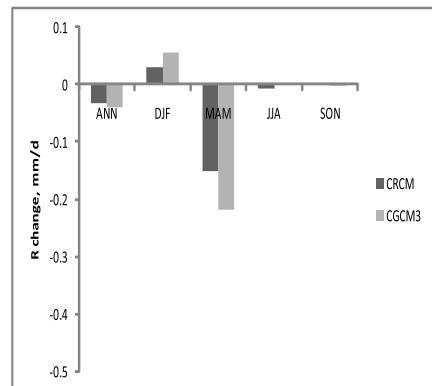
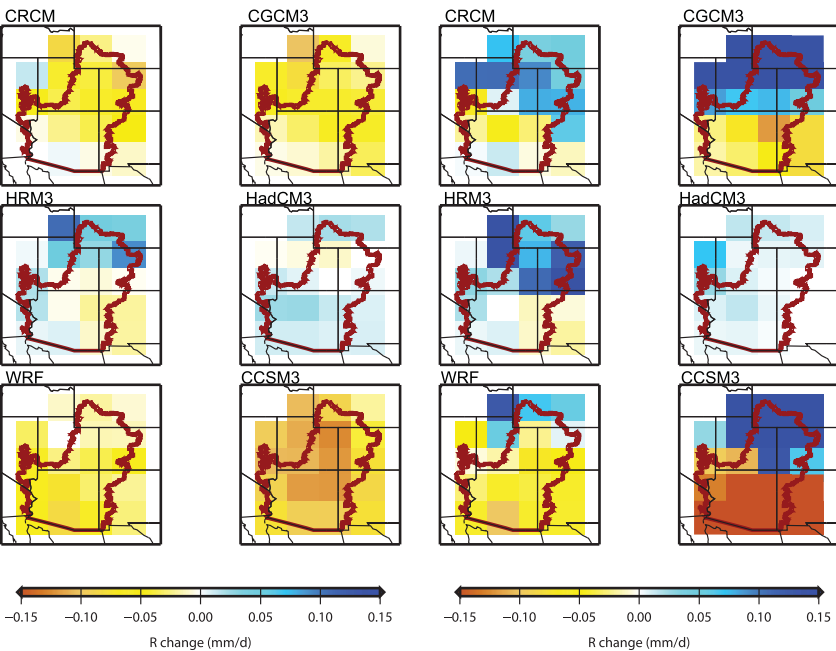
SWE change (mm)



SWE change (mm)

ANN

DJF



MAM

JJA

